J Electroceram (2007) 19:47–65
DOI 10.1007/s10832-007-9001-1

Domain wall contributions to the properties of piezoelectric thin films

Nazanin Bassiri-Gharb · Ichiro Fujii · Eunki Hong · Susan Trolier-McKinstry · David V. Taylor · Dragan Damjanovic

Received: 27 September 2006 / Accepted: 15 January 2007 / Published online: 8 March 2007

Abstract In bulk ferroelectric ceramics, extrinsic contributions associated with motion of domain walls and phase boundaries are a significant component of the measured dielectric and piezoelectric response. In thin films, the small grain sizes, substantial residual stresses, and the high concentration of point and line defects change the relative mobility of these boundaries. One of the consequences of this is that thin films typically act as hard piezoelectrics. This paper reviews the literature in this field, emphasizing the difference between the nonlinearities observed in the dielectric and piezoelectric properties of films. The effect of ac field excitation levels, dc bias fields, temperature, and applied mechanical stress are discussed.

N. Bassiri-Gharb · I. Fujii · E. Hong · S. Trolier-McKinstry
Materials Research Institute, The Pennsylvania State University,
University Park, PA 16802, USA

N. Bassiri-Gharb · I. Fujii · E. Hong · S. Trolier-McKinstry
Materials Science and Engineering Department,
The Pennsylvania State University,
University Park, PA 16802, USA

D. V. Taylor · D. Damjanovic
Ceramics Laboratory,
Swiss Federal Institute of Technology (EPFL),
Lausanne, Switzerland

N. Bassiri-Gharb (✉)
Materials and Device R&D,
QUALCOMM MEMS Technologies, Incorporated,
2581 Junction Ave., 120.I.,
San Jose, CA 95134, USA
e-mail: nazaninb@qualcomm.com

Present address:
D. V. Taylor
Nanosys Inc., Palo Alto, CA 94304, USA

Keywords Review · Domain walls · Piezoelectric thin films

1 Introduction

With their superior dielectric and piezoelectric response, perovskite-structured ferroelectric thin films have attracted attention for application in capacitors and microelectromechanical systems (MEMS). The large dielectric response of these materials is due in part to intrinsic (averaged crystallographic response of the ferroelectric material's domains) and in part due to extrinsic contributions, mainly due to the motion of the domain walls and phase boundaries. In perovskite ferroelectrics, domain walls can be moved by electric fields, stresses, or combinations of the two. Indeed, domain wall motion is the process by which the spontaneous polarization is oriented during poling processes to yield a net piezoelectric effect. Domain wall motion is an important contributor to the dielectric response of polycrystalline ceramic materials, and is a major component of the extrinsic piezoelectric response [1]. Extrinsic contributions can be responsible for up to ~75% of the dielectric and piezoelectric response of a ferroelectric ceramic [2]. However, while domain wall motion is extremely useful in increasing the achievable response, the walls move through a potential field that can locally pin the walls, for example due to local elastic or electric fields. Motion is thus a progressive process of freeing, moving, and re-pinning the walls. As a result, domain wall motion is hysteretic and nonlinear. Due to extrinsic contributions, the effective dielectric and piezoelectric coefficients of ferroelectrics depend on the applied electric field strength and frequency [2]. As many applications require thinner films (sensors and actuators in MEMS, multilayer capacitors, etc.) an understanding of the

high field response of ferroelectrics becomes crucial for prediction of the device behavior. The AC electric field dependence of the dielectric permittivity and piezoelectric response of ferroelectric thin films in sub-switching conditions can be described using a Rayleigh-type approach [3–5]. In this paper, domain wall contributions to the dielectric response of ferroelectric thin films will be discussed. Following that, the extrinsic contributions to thin film piezoelectric response will be covered.

2 Background

In a ferroelectric material, the distortion of the unit cell at the Curie temperature (T_C) is accompanied by the creation of a spontaneous polarization and an accompanying strain. On cooling to temperatures lower than T_C, the material tends to reduce its total energy by creating domain structures [6]. Domains are volumes of material where the polarization direction is uniform (or at least nearly so) [7]. The dielectric and piezoelectric response of ferroelectric ceramics are usually due to the average response of the single domains present in the ceramic (intrinsic), and contributions due to the motion of the domain walls and phase boundaries and displacement of defects, these latter constituting the so called "extrinsic contributions" [8, 9].

One method used to distinguish between the intrinsic and the extrinsic contributions to the properties of a ferroelectric is the study of the field amplitude dependence of the response [2]. Typically the relative dielectric permittivity ε_r is defined as the proportionality constant in the linear relationship between dielectric displacement D and electric field E [6]. It has been reported for a number of ferroelectric ceramics and thin films that this linear relationship doesn't hold beyond a certain threshold field E_{th} (See Fig. 1) [10]. At increasing ac field levels, in fact, ε_r becomes a function of the applied field's amplitude. This phenomenon is usually referred to as dielectric nonlinearity (i.e. a nonlinear relationship between D and E). Analogous behavior has been also observed for piezoelectric coefficients dependence on driving fields (piezoelectric nonlinearity).

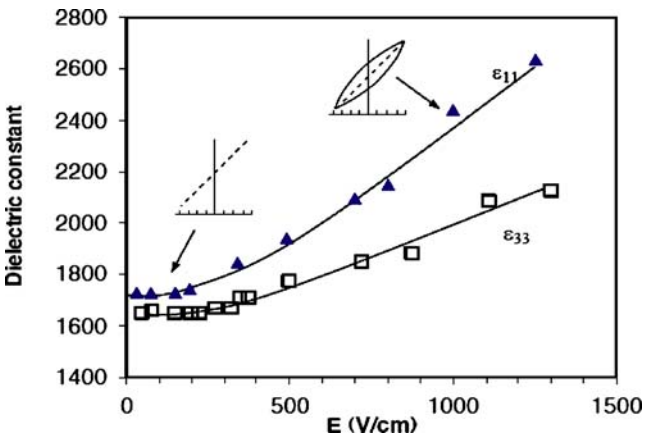

Fig. 1 The nonlinear behavior of the dielectric permittivities ε_{11} and ε_{33} with the applied AC field in a soft PZT ceramic, after [10]

The nonlinear response has, in principle, both intrinsic and extrinsic components. The intrinsic nonlinearity can be modeled using a Landau–Ginzburg–Devonshire approach [11, 12]. In most cases, because the working conditions of the device are at ac field values below the coercive field, the intrinsic nonlinearities are comparatively small and therefore, the dominant nonlinearity in bulk ferroelectric perovskite ceramics is assumed to be extrinsic in origin. The behavior of the dielectric permittivity and piezoelectric coefficients for ac field amplitudes higher than E_{th} can, in many cases, be described by the Rayleigh Law.

The Rayleigh law, originally applied to ferromagnetic materials [13], can describe the macroscopic effects of hysteretic motion of interfaces across a random potential energy landscape [14]. In the case of ferroelectrics, the Rayleigh Law translates into a *linear* ac electric field dependence of the permittivity and piezoelectric coefficients in sub-switching conditions, where the density and the structure of the domain walls remain unchanged with field cycling [15]. At still higher fields, the field dependence of the dielectric permittivity can become super- or sub-linear due to the change in the domain wall motion potential energies and, in general, polarization switching [15]. The onset of this "high field" region usually corresponds to 1/3–1/2 of the coercive field [15].

The Rayleigh Law applied to the nonlinear dielectric response can be written as:

$$\varepsilon^* = \varepsilon' - j\varepsilon \qquad \text{(complex dielectric permittivity)} \tag{1}$$

$$|\varepsilon^*| = \sqrt{(\varepsilon')^2 + (\varepsilon)^2} = \varepsilon_r \quad \text{(dielectric permittivity)} \tag{2}$$

$$\varepsilon' = \varepsilon'_{init} + \alpha' E_0 \qquad \text{(real dielectric permittivity)} \tag{3}$$

$$P(E) = \left(\varepsilon'_{init} + \alpha' E_0\right) E \pm \frac{\alpha'}{2}\left(E_0^2 - E^2\right) \tag{4}$$

$$P(E) = \left(\varepsilon'_{init} E_0 + \alpha' E_0^2\right) \sin(\omega t) + \frac{4\alpha' E_0^2}{3\pi} \cos(\omega t) + \frac{4\alpha' E_0^2}{15\pi} \cos(3\omega t) - \frac{4\alpha' E_0^2}{105\pi} \cos(5\omega t) + \ldots \tag{5}$$

where P is the dielectric polarization, E_0 is the amplitude of the driving field $E=E_0 \sin(\omega t)$, ε'_{init} and α' are the reversible and irreversible Rayleigh coefficients, respectively, and all permittivity values are relative to vacuum. Note that Eq. 5 implies only odd order harmonics of polarization dependence on electric field. The reversible Rayleigh coefficient

is due to contributions from the intrinsic lattice and reversible motion of the interfaces. The irreversible domain wall or phase boundary displacements contribute to the dielectric response through the $\alpha' E_0$ term. At a fixed field, therefore, the ratio of the irreversible to reversible Rayleigh parameters represents a measure of the extrinsic contributions to the dielectric properties of the material. Since the nonlinear dielectric response is dominated by extrinsic contributions mainly due to interface motion, which is a thermally activated phenomenon [16], the field dependence of the dielectric permittivity should also be a function of the temperature.

In the same way, motion of non-180° domain walls is a significant contributor to the piezoelectric coefficients. Typically, in bulk material, these extrinsic contributions dominate the measured piezoelectric nonlinearity, hysteresis, and the frequency dependence of the piezoelectric response. The Rayleigh relations analogous to Eqs. 1, 2, 3, and 4 can be written for the piezoelectric effect [15]. Variations on Eq. 5 for piezoelectric effect will be discussed in further detail in section 4.

The dielectric and piezoelectric properties of many bulk ceramics [2, 15, 17] and polydomain single crystals [18] exhibit Rayleigh-like behavior. Important exceptions are acceptor doped or hard piezoelectric materials [15, 19]. To understand why the experimentally observed nonlinearity can depart from equations (3–4), it is necessary to discuss in some detail the meaning of the Rayleigh relations. The most important feature of these relations is that they link the hysteresis (irreversible behavior) and nonlinearity, through the parameter α'. In other words, the same mechanism in the material is responsible for the nonlinearity and the hysteresis for the driving fields over which Rayleigh behavior is observed. Furthermore, the derivation of the relations does not imply any rate-dependent or thermally activated processes [14, 20] Finally, these relations imply that a domain wall or an interface moves in a random potential; this last statement becomes obvious when Rayleigh relations are derived in the framework of the Preisach model [15, 21].

It is clear that Rayleigh relations may hold only approximately and over a limited field range. In a real material the distribution of pinning potential parameters may significantly depart from the randomness necessary for ideal Rayleigh behavior. This leads to either the appearance of threshold fields for the onset of nonlinearity and/or sublinear or super-linear dependence of the dielectric or piezoelectric coefficients on the driving field amplitude [21, 22]. One can speak of Rayleigh-like or modified Rayleigh behavior, where the essential link between the hysteresis and nonlinearity can be easily introduced by allowing α' to be field dependent [15, 21, 22]. It should be emphasized that in such cases only the statistical properties of the potential energy profile seen by the moving interface change; the physical mechanism (domain wall pinning) remains the same as in the case of the ideal Rayleigh behavior.

Clearly, other non-Rayleigh mechanisms may operate in a material. For example, oscillations of domain walls in a viscous environment or dipole-like reorientation of domain walls may give a rate-dependent hysteresis without nonlinearity [15, 23]. In those cases, the experimental hysteresis is larger than that predicted from the nonlinearity in the permittivity or the piezoelectric coefficient, and one can effectively separate linear and nonlinear contributions to the hysteresis [17, 25]. In contrast to cases where Rayleigh behavior dominates the total response, in well aged acceptor-doped (or hard) PZT ceramics the weak field nonlinearity is dominated by a nonhysteretic process; therefore, the nonlinearity and the small hysteresis cannot be linked through Rayleigh relations or their modifications [15, 24]. To summarize, analysis of nonlinearity alone is not sufficient to verify whether a Rayleigh-like process is present in the material; the link between nonlinearity and hysteresis must be established. For this purpose, analysis of the higher harmonics in the response appears to be essential [15, 24]. An example of experimental confirmation of a link between the hysteresis and nonlinearity for the dielectric response of a $Pb(Zr,Ti)O_3$ thin film is given in Fig. 2.

Often, several mechanisms may operate in the material simultaneously and their identification and separation may be very challenging [25]. For the present purposes, whenever the dominant material response may be approximately described by the Rayleigh relations, other mechanisms are neglected.

Analysis of the dielectric and piezoelectric response using Rayleigh relations has been used successfully in the past to obtain information on domain wall contributions in bulk materials [2]. Rayleigh relations describe nonlinearity and hysteresis well in soft $Pb(Zr,Ti)O_3$ (PZT) ceramics [2, 17] but, as mentioned above, are not applicable to all acceptor doped or hard materials (e.g., Fe-doped PZT) [15, 24]. Nevertheless, even in acceptor-doped PZT the hysteresis and nonlinearity decrease as the material becomes harder, just as one would expect from progressively stronger pinning of domain walls in a soft material. In tetragonal PZT compositions, the irreversible Rayleigh parameter α' peaks at the MPB [26], confirming the empirical result that domain wall contributions are maximized at the MPB. The behavior on the rhombohedral side of the MPB is more complex. In rhombohedral ceramics the parameter α' remains high away from the MPB. A possible reason for this difference between tetragonal and rhombohedral compositions is that in compositions with a high tetragonality, the domain wall displacement is reduced because of the internal stresses associated with the high spontaneous strain. The role of internal stress was also

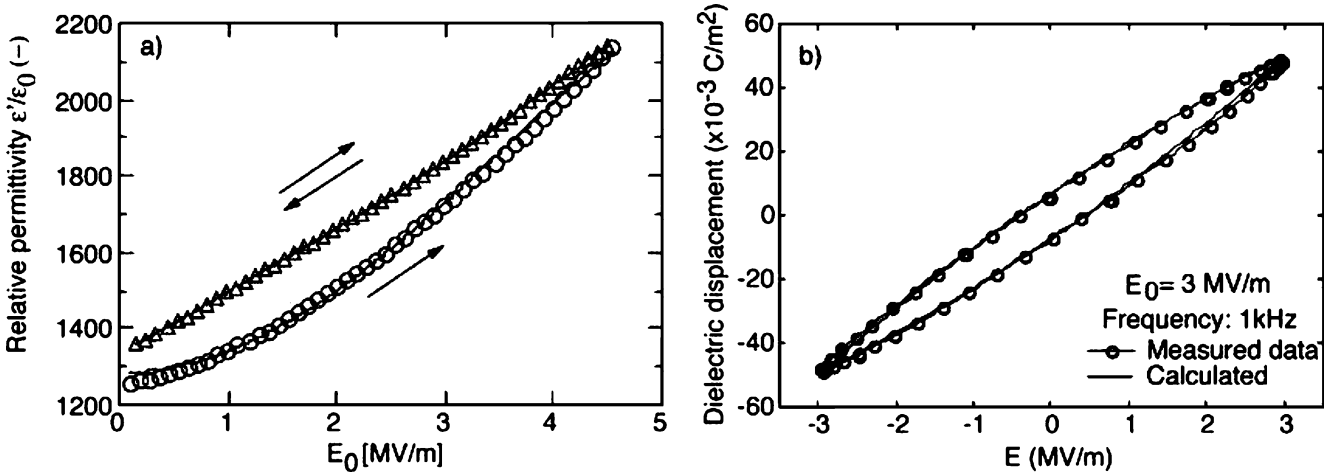

Fig. 2 Illustration of the link between the nonlinearity and hystersis, one of the salient features of Rayleigh-like behavior, in a 1.44 μm thick (111) oriented 45/55 PZT film. (**a**) relative permittivity for increasing and decreasing amplitude of the driving field. (**b**) Measured and calculated polarization loop of the same film, for decreasing branch. The calculated loop is determined using nonlinear parameters of the permittivity in (**a**) and relations (3–4). For details see [3, 4, 78]

invoked to explain differences in the piezoelectric nonlinearity and hysteresis between coarse and fine grain $BaTiO_3$ ceramics [26].

The nature of the pinning centers for ferroelectric domain walls is not well understood. This is true even for classical materials such as acceptor doped $BaTiO_3$ [27] and PZT. In acceptor doped PZT, both hysteresis and nonlinearity were examined, and it was found that well aged ceramics cannot be described by Rayleigh relations [24]. As explained in Ref. [15], the potential energy profile for a domain wall in an acceptor doped material is not random but *V*-shaped. Displacement of the domain walls is nonlinear and exhibits only a small hysteresis, indicating that local traps for the domain walls are few and shallow. This form of the potential is the consequence of alignment of defect dipoles with the polarization on each side of the domain wall [28]. As a consequence, for a well-aged PZT ceramic, if the polarization—electric field minor loop is calculated from the α' determined from the field dependence of the permittivity, the calculated loop has too large an area. This means that there is a contribution to the nonlinearity that is not hysteretic—and that this contribution can be bigger than the hysteretic part. In addition, the phase angle of the third harmonic in hard PZT did not follow a Rayleigh prediction. In Fe-doped $BaTiO_3$, Boser [29], who derived Rayleigh relations for the dielectric response of ferroelectrics following the statistical approach of Kronmüller [20], used the field dependence of the permittivity from [30] to support the theoretically derived dependence of α' on defect concentration. However, Boser did not verify the link between the hysteresis and nonlinearity in the experimental data analyzed. Thus, it is difficult to accept the claim that the theoretically-derived dependence of α' on defect concentration was experimentally confirmed. The effect of elastic defects and microstructure on the direct piezoelectric effect of Aurivillius structured compounds [31] has been analyzed in the framework of the Rayleigh approach, taking into account both the hysteresis and nonlinearity.

Finally, the Rayleigh approach was used to analyze domain wall contributions to the direct piezoelectric effect in relaxor-ferroelectric $x\mathrm{Pb}(\mathrm{Zn}_{2/3}\mathrm{Nb}_{1/3})\mathrm{O}_3$–$(1-x)\mathrm{PbTiO}_3$ single crystals with engineered domain structures. In this case, where ferroelastic domain wall motion is not expected, the dominant response is intrinsic. However, non-negligible modified Rayleigh behavior was observed [32].

In summary, one can say that many families of ferroelectric ceramics and single crystals exhibit significant extrinsic nonlinearity and hysteresis, which, in many but not in all cases, may be described by the Rayleigh-like approach. Knowledge of the extrinsic contributions in thin films is less extensive than in bulk materials and, as discussed below, a simple extrapolation of results obtained in bulk materials to thin films is not always possible.

First of all, it is important to recognize that thin films may have very different potential profiles for the moving domain walls than bulk ceramics, as reviewed elsewhere [33]. One result of this is that the coercive fields for ferroelectric thin films significantly exceed (often by an order of magnitude) those of bulk materials of the same composition. There are many possible reasons for this. For example, the grain sizes in thin films are typically small (e.g. 50–250 nm), while bulk ceramics in general have much larger grain sizes (on the order of microns). This has the effect of both introducing a high density of grain boundaries, and increasing the density of domain walls [34]. Closely spaced walls may interfere with each other's motion, lowering the domain wall mobility [35], as has been reported for fine grain $BaTiO_3$ ceramics [26]. In addition, thin films are susceptible to large concentrations of point and line defects. Indeed, in thin films, it is not uncommon for ABO_3 perovskites to be

stabilized at A:B ratios that would lead to phase separation in the bulk, which could lead to large point defect concentrations. It is well known in bulk lead zirconate titanate ceramics that changes in the defect dipole concentrations modulate the extent of extrinsic contributions to the properties [36]. Recently, it has been predicted that dislocations impede motion of 90° domain walls, and so should be expected to reduce extrinsic contributions to the properties of epitaxial thin films [37]. Finally, thin films are often under substantial levels of residual stress that can change the ferroelastic domain population [38]. Because grain boundaries, nearby domain walls, defect dipoles, and local stresses can act as pinning sites for domain walls, it is not immediately obvious that the domain wall contributions to the properties will be identical for thin film and bulk ferroelectrics of the same composition.

Tuttle et al. were among the first to report on the observation that non-180° domain wall motion is substantially smaller in PZT thin films than in bulk ceramics of the same composition [39]. They reported that the domain structure was strongly influenced by the sign of the stress experienced by the film on cooling through the ferroelectric phase transition. Those films in tensile stress at T_C (e.g. most perovskite films on Si substrates) have a propensity for the polarization to lie in-plane, particularly in fine-grained samples. It was found that permanently reorienting the polarization was difficult with applied electric fields. In many cases, applied tensile stresses are found to rotate the polarization hysteresis loop clockwise, while compressive stresses rotate it counterclockwise [42, 44], which is consistent with the observation that thin films under tensile stress typically have substantially smaller remanent polarizations than those in compressive stress. Lee et al. reported that in PZT 32/68 films it was possible to switch ~2 vol.% of the film between a and c orientations with applied electric fields exceeding the coercive field. When the electric field was removed, the domain population largely recovered to its original value [40]. Kelman et al. have demonstrated that in tetragonally distorted PZT 35/65 thin films, about 5% of the film underwent 90° domain switching under the combined influence of applied in-plane tensile stresses and applied fields [41]. In contrast, for subcoercive electric field excitations, low levels of ferroelastic domain wall mobility are reported for applied dc stresses for several perovskite ferroelectric films [42–44]. In most cases, comparatively low levels of non-180° domain wall motion (certainly well below those shown by bulk ceramics of the same composition) can be driven by ac electric fields alone in films under a micron in thickness [45, 46]. Similar conclusions have been drawn for $SrBi_2Ta_2O_9$ films [47].

As the film thickness rises, it has been reported that domain wall motion contributes more to the observed room temperature permittivity and piezoelectric coefficients [16]. For example, it has been observed that for some PZT thin films, the room temperature permittivity is a strong function of thickness, with thicker films showing much larger values. However, the thickness dependence largely disappears when the samples are cooled to 4 K. This is consistent with the observation that domain wall motion is thermally activated; thus the differences in room temperature permittivity were associated with extrinsic effects, which increased as the film thickness rose. Likewise, it was shown that the likelihood of permanent reorientation of ferroelastic domains by application of bias fields increased with the thickness and grain size of the films [16].

The dielectric and piezoelectric properties of epitaxial ferroelectric films with dense laminar domain structures were calculated by Koukhar et al. [38] and Pertsev and Emelyanov [48]. It was shown that the domain structure is mainly controlled by the misfit strain between the substrate and the film and a large enhancement of the response is predicted for certain values of the misfit strain. In the terminology of the Rayleigh relations, the calculated contributions lead to an increase in d_{init}. These approaches do not consider nonlinearity and hysteresis of the electromechanical response and will not be further discussed.

3 Quantifying the dielectric response as a function of ac electric field

As described above, the Rayleigh approach can be used to quantify the irreversible extrinsic contributions to the dielectric and piezoelectric properties of ferroelectrics. Denominations like “soft” and “hard” have been historically used in the literature to distinguish the properties of doped PZT samples with different levels of pinning of the domain walls. Table 1 compares the Rayleigh parameters and the ratio of the irreversible to reversible Rayleigh parameters for the dielectric response of a variety of bulk and thin film ferroelectrics. The values were obtained by fitting the linear portion of the data for the measured permittivity as a function of the amplitude of the ac electric field. As expected, soft PZT ceramics show much larger nonlinearity than hard PZTs. This is reflected in the observation that the irreversible Rayleigh parameters (and the ratio of the irreversible to reversible Rayleigh parameters) are one order of magnitude smaller for the hard PZT compositions with respect to the soft compositions. Moreover, for the same composition, films are harder than hard ceramics, so that the dielectric $\alpha'/\varepsilon'_{init}$ ratio is even lower in films than in ceramics. It is believed that the smaller average grain size of thin films than ceramics, the higher defect concentration, and clamping to the substrate yield a lower concentration of mobile interfaces, which lowers extrinsic contributions to the

Table 1 Comparison of the Rayleigh coefficients for the dielectric response of various ferroelectric ceramics and thin films.

Composition	Sample	Orientation	ε'_{init}	α' (cm/kV)[b]	$\alpha'/\varepsilon'_{init}$ (cm/kV)	Reference
Ferroperm PZ26	(Hard) ceramic		1,365	67[b]	0.049	[50]
soft PZT	Ceramic		1,820	320	0.18	[51][a]
PZT Zr:Ti=58:42	Ceramic		530	130	0.25	[24][a]
PZT Zr:Ti=58:42+0.2% Nb	Ceramic		540	305	0.56	[24][a]
soft PZT	Ceramic		1,450	900	0.62	[10][a]
PZT Zr:Ti=45:55	Film,1.3 μm	(111)	888	7.8	0.0088	[3]
PZT Zr:Ti=45:55	Film,1.5 μm	(111)	1,340	13	0.0097	[4][a]
PZT Zr:Ti=45:55	Film		890	18	0.020	[52][a]
PZT Zr:Ti=52:48	0.9 μm thick film	(100) Unpoled	1,288±13	38.2±0.2	0.03±0.002	
PZT Zr:Ti=52:48	0.9 μm thick film	(100) Poled	1,098±9	36.3±0.3	0.033±0.002	
PZT Zr:Ti=52:48	0.9 μm thick film	(111) Unpoled	1,097±10	28.2±0.3	0.026±0.001	
PZT Zr:Ti=52:48	0.9 μm thick film	(111) Poled	980±20	22.0±2.0	0.024±0.002	
PMN–PT	1 μm thick film	(100) Unpoled	2,060±11	61.5±0.4	0.030±0.002	
PMN–PT	1 μm thick film	(100) Poled	2,042±8	58.2±0.4	0.029±0.002	
PMN–PT	0.6 μm thick film	(111) Unpoled	1,746±23	40.2±0.2	0.023±0.001	
PMN–PT	0.6 μm thick film	(111) Poled	1,625±13	32.2±0.3	0.020±0.002	
PYbN–PT	0.6 μm thick film	(111)	1,036±20	14.1±0.1	0.014±0.0005	[60]
$PbTiO_3$	0.26 μm thick film	{100} and {111}	340±2-	3.25±0.5	0.0096±0.002	[53]

Data given without a specific reference were measured by the authors.
[a] Extrapolated data
[b] For hard ceramics, the symbol α' is used to describe the nonlinearity only. The Rayleigh relations do not necessarily hold, but the low α, representing nonlinearity, does indicate reduced extrinsic contributions.

dielectric constant in thin films. As will be described in more detail below, the α' values increase with increasing thickness for films of the same composition and orientation.

It should be emphasized that the terms "soft" and "hard" as applied to ferroelectrics should be used with care. Depending on context, these terms may indicate one of two things. In a more narrow sense, the term "hard" is reserved for acceptor-doped materials where the piezoelectric, dielectric, and compliance coefficients (with their associated nonlinearity, hysteresis and frequency dependence) are reduced, while the coercive field is increased with respect to undoped material. An example is Fe-doped PZT [36] where the hardening is associated with the presence of defect dipoles. For materials *in a well aged state*, there is evidence, as mentioned above, that Rayleigh relations do not hold (Instead, the material evolves during the measurement, so that Rayleigh behavior becomes progressively more apparent) [19, 24]. This is similar to the process sometimes referred to in the literature on magnetics as "training" of the material [49]. In the more general sense used here, the term "hard material" refers to ferroelectrics that exhibit reduced elastodielectric properties, require high poling fields and exhibit large coercive fields, but the hardening is not necessarily achieved by doping. A good example is most undoped PZT films with an MPB composition. The films exhibit lower electromechanical response and higher coercive field with respect to bulk ceramics of the same composition; the effective hardening, however, is not caused by presence of deliberately incorporated acceptor dopants, but is rather related to microstructural parameters including a smaller grain size, clamping by the substrate, and high defect density. In such a case, the Rayleigh approach might be used to describe the extrinsic contributions to electromechanical properties, once the essential link between the hysteresis and nonlinearity is verified. When acceptor dopants are not deliberately added, it is still possible to have a non-negligible concentration of $V_{Pb''}-V_{O^{\cdot\cdot}}$ defect dipoles in the films. If these dipoles behave in the same way as acceptor dopant-oxygen vacancy dipoles, only part of the observed nonlinearity may be of Rayleigh type.

3.1 Effect of dc electric field on domain wall motion and dielectric response

As a dc electric field parallel to P_r is applied to a ferroelectric, the domain state is stabilized and the density of domains walls may be reduced. The impact of this on the ac field dependence of the dielectric constant is illustrated in Fig. 3 for a pre-poled {100} oriented $0.5PbYb_{1/2}Nb_{1/2}O_3$–$0.5PbTiO_3$ film. The Rayleigh region extends over a much wider field range as dc bias is applied, and the ac field dependence of the dielectric response is considerably flattened. This occurs because the applied bias should further pole the material and stabilize the domain structure, retarding the onset of depoling and switching. It can be seen that the

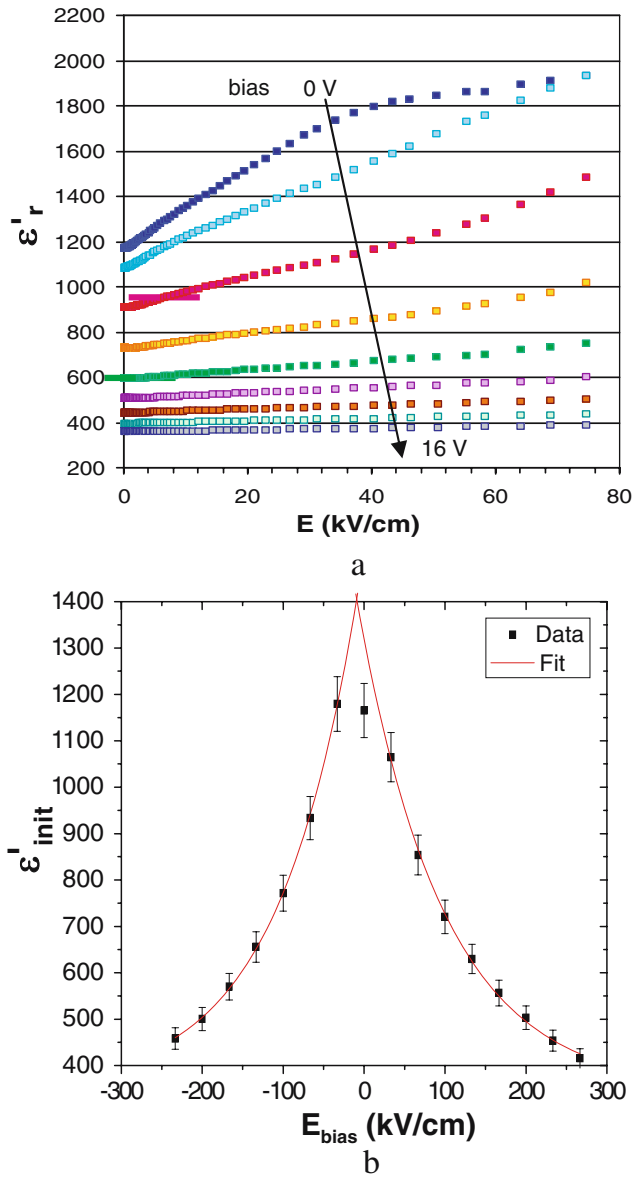

Fig. 3 Effect of dc bias field (**a**) on dielectric constant (**b**) on $\varepsilon'_{\text{init}}$ for (100) oriented $0.5PbYb_{1/2}Nb_{1/2}O_3$–$0.5PbTiO_3$ films

bias field dependence can be well fitted with an exponential decay:

$$\varepsilon'_{\text{init}} = (345 \pm 18) + (973 \pm 40)\, e^{[(-0.0094 \pm 0.0006) E_{\text{bias}}]}$$

where E_{bias} is the applied bias field in kV/cm. The same functional form could also be used to fit α' and the ratio $\alpha'/\varepsilon'_{\text{init}}$. This exponential drop in the permittivity with bias differs from predictions from phenomenological theory: [54] $\varepsilon = 1/(-\xi T + 3(\psi E_{\text{bias}})^{2/3})$ where T is the temperature at which the measurements are performed and ξ and ψ are two constants of the material, related to the free energy, non-linear dielectric coefficients of the material and the Curie temperature. The discrepancy arises because the phenomenological model describes only the intrinsic response, and so does not account for domain wall motion.

The inadequacy of the phenomenological model has been also reported by Ang et al. [55] The authors showed for PZT thin films that the phenomenological theory provided a relatively good fit at cryogenic temperatures. With increasing temperature, the phenomenological model was progressively less accurate, until at room temperature, it accounted for less than 50% of the experimental dielectric constant observed at intermediate fields. The same authors suggested a "reorientational polar cluster" model to describe the extrinsic contributions [56]. The comprehensive expression is mathematically complex, but is valid only at small polarization values (≤5 μC/cm^2). The exponential expression given here for the bias field dependence of the Rayleigh parameters and their ratio applies over a wide range of bias fields and is mathematically simple.

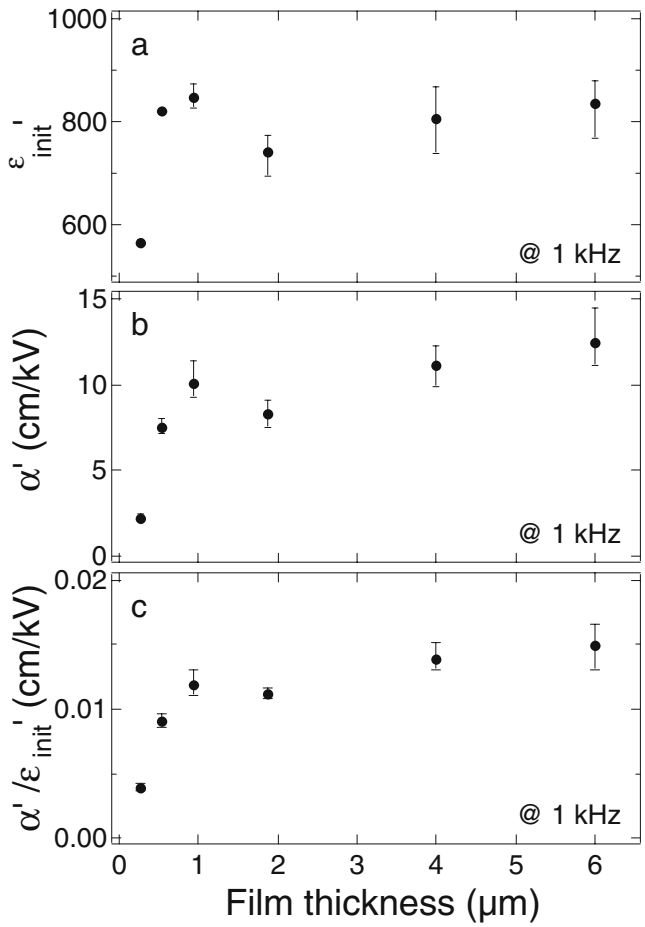

Fig. 4 (**a**) $\varepsilon'_{\text{init}}$, (**b**) α', and (**c**) the ratio $\alpha'/\varepsilon'_{\text{init}}$ for PZT films as a function of film thickness

Table 2 Frequency dependence of nonlinearity in PZT 52/48 thin films as a function of thickness.

Thickness (μm)	ε'_{init}		α' (cm/kV)		$\alpha'/\varepsilon'_{init}$ (cm/kV)	
	A	*B*	*A*	*B*	*A*	*B*
0.26	600.4	12.4	2.5	0.1	0.0041	0.0002
0.53	916.4	29.7	8.8	0.6	0.0097	0.0005
0.93	928.8	29.6	11.6	0.8	0.0126	0.0006
1.87	840.5	29.5	10.7	0.8	0.0129	0.0006
4.00	958.7	31.6	14.9	1.2	0.0158	0.0009
6.00	974.1	32.8	18.6	1.4	0.0193	0.0009

3.2 Effect of film thickness on domain wall motion

Sol-gel derived PZT (Zr/Ti=52/48) films with thicknesses t=0.26, 0.53, 0.93, 1.87, 4, and 6 μm were prepared by a chemical solution deposition process on Pt-coated Si substrates as described elsewhere (excepting that a 0.4 M solution was used for the 0.26 μm thick film) [57, 58]. All of the films showed a Rayleigh region for the dielectric permittivity. It was found that as the film thickness increased, the Rayleigh region extended over a smaller range of field amplitudes, tracking the thickness dependence of the coercive field for the films. That is, as the film thickness increased, the potential profile energy for moving domain walls appears to be either skewed towards more shallow wells, or that the concentration of pinning sites is lower and the ac electric field required to change the density or structure of the domain walls decreased.

As shown in Fig. 4, the Rayleigh parameters increased with increasing film thickness up to about 1 μm and then saturated. Thus, domain wall motion is apparently reduced for film thicknesses below 1 μm. This is also reflected in the frequency dependence of the Rayleigh parameters, as shown in Table 2, where A and B are constants for a general decay law:

$$y = A - B \log f \text{ for frequencies in Hz.}$$

It can be seen that for the thinner films there is less frequency dependence in the dielectric response due to domain wall motion.

There are several possible explanations for the thickness dependence, including a change in the concentration of mobile domain walls as film thickness drops, or the presence of non-ferroelectric material. If a second phase is present, either distributed through the film, or localized at the electrode/film interface (e.g. a passive or "dead" layer) then the measured ac field dependence of the response will be diluted. The net result would be an apparent decrease in both the Rayleigh parameters and their frequency dependence. To ascertain which of these effects was dominant, the ac field dependence of the dielectric constant was also measured at different dc biases. In all cases, a Rayleigh region was observed, and the extent of the Rayleigh region increased with dc-bias as discussed above. Figure 5 shows the dc bias dependence of ε'_{init}, α', and $\alpha'/\varepsilon'_{init}$. It was found that these parameters increased with increasing dc bias up to about the coercive field and then decreased for dc biases over E_c. For the 0.26 μm thick film, it was observed that the increase in α' was small. This suggests that the contribution of domain wall motion to the dielectric constant is small. It is also important to note that the convergence of ε'_{init} and α' at high dc biases for all thicknesses suggests that the thickness dependence noted at small fields is probably due primarily to domain wall

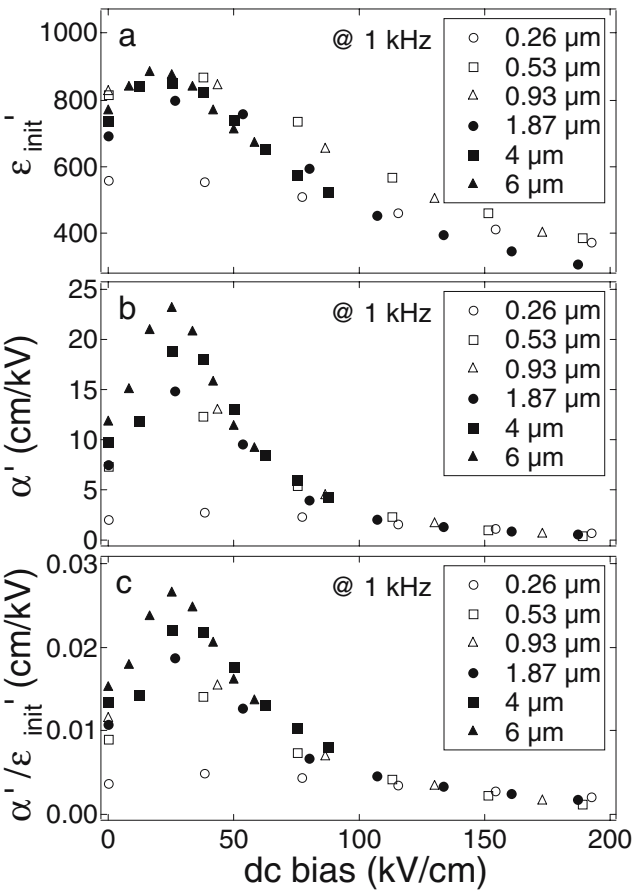

Fig. 5 (**a**) The reversible Rayleigh coefficient, ε'_{init}, (**b**) the irreversible Rayleigh coefficient α', and (**c**) the ratio $\alpha'/\varepsilon'_{init}$ for the PZT films as a function of frequency

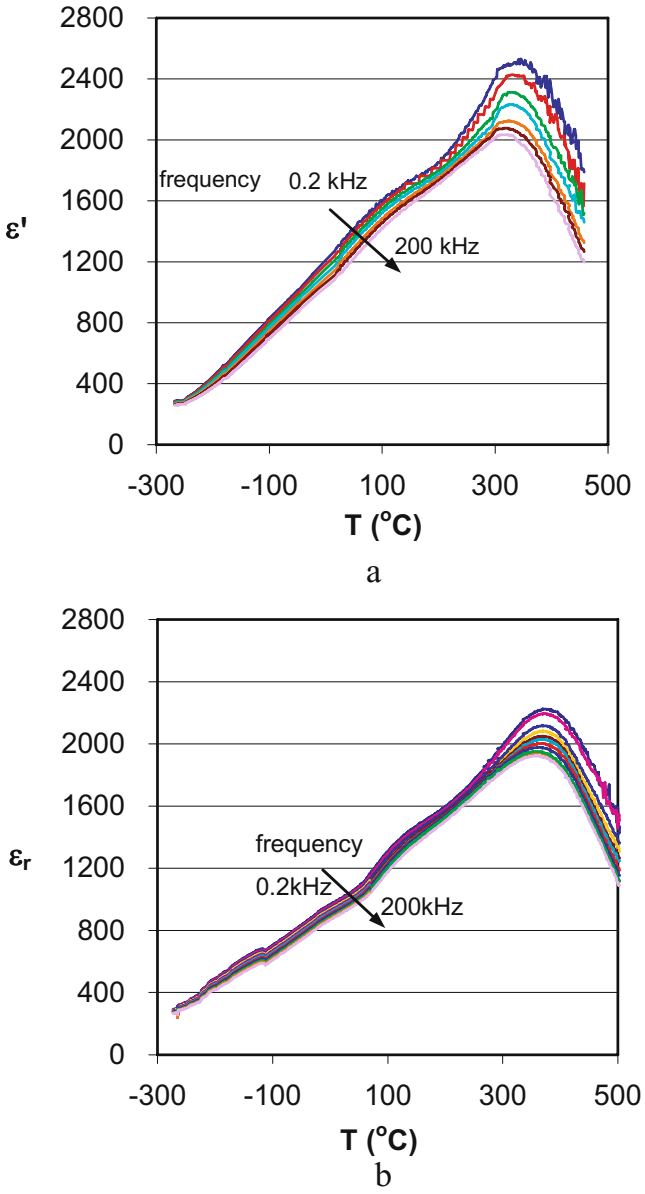

Fig. 6 Temperature dependence of dielectric permittivity for (**a**) {100} oriented and (**b**) {111} oriented PYbN–PT films at low fields ($<E_{th}$). The reported curves correspond to frequencies between 200 Hz and 200 kHz

motion, rather than to the existence of a low permittivity interfacial layer, which should depress the measured permittivity for all dc bias fields.

3.3 Effect of temperature on domain wall motion

Rayleigh-like hysteresis and nonlinearity are activated by the driving field. However, it is well known that domain wall and phase boundary motion are also thermally activated phenomena [59]. Thus, at high enough temperatures, field and thermal effects will couple. To demonstrate the effect of temperature and phase transitions on domain wall motion and Rayleigh relations in thin films, $0.5Pb(Yb_{1/2}Nb_{1/2})O_3$–$0.5PbTiO_3$ (PYbN–PT) films were investigated. Sol–gel derived 0.5PYbN–0.5PT films with preferential {111} and {100} crystallographic orientation were grown on platinized silicon substrates. The thicknesses of the films were approximately 0.67 and 0.62 μm and the grain size was in the 30–45 nm and 200–300 nm range respectively for the {111} and {100} oriented films. Further details on processing and characterization of these films are reported elsewhere [60].

Table 3 Nonlinear dielectric properties of the as-deposited films at room temperature.

Sample	ε'_{init}	α' (cm/kV)	$\alpha'/\varepsilon'_{init}$ (cm/kV)
{100}	1,212	19.8	0.016
{111}	874	16.8	0.019

All the values are subject to 5% experimental error.

Peaks in dielectric permittivity as a function of temperature were observed at ~380°C, corresponding to T_C (See Fig. 6). Smaller shoulders were also observed at ~140°C, suggesting a rhombohedral to tetragonal phase transformation, which is consistent with curvature in the morphotropic phase boundary. The dielectric loss decreased monotonically up to temperatures around 250°C. At higher temperatures, the loss tangent increased rapidly, which is probably due in part to the increased conductivity levels in the films. {100} oriented films showed higher dielectric loss than the {111} oriented films over the studied temperature range.

To minimize artifacts associated with aging [61], the temperature dependent dielectric nonlinear measurements were performed without poling the samples and at 1 kHz.

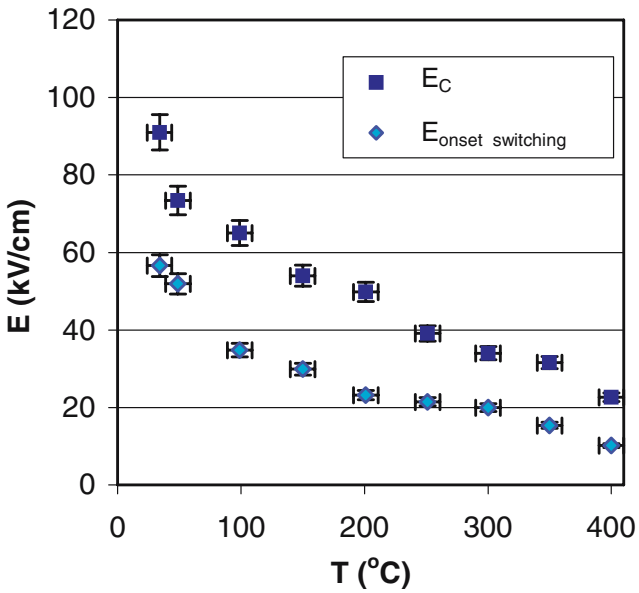

Fig. 7 Temperature dependence of the high field region onset for a {111} oriented PYbN–PT film at 1 kHz

The accuracy of this temperature for the nonlinear sweep was approximately 5–6%. The characteristic dielectric nonlinear properties of the films at room temperature are reported in Table 3.

As shown in Fig. 7, the onset for the high field region (the point at which the permittivity versus ac field amplitude departed from linearity), as well as the coercive field decreased with increasing temperature. This occurs because domain wall motion and polarization reversal are facilitated at higher temperatures [62]. The final effect was that of decreasing the width of the ideal Rayleigh region, as shown in Fig. 8.

The temperature dependence of the reversible and irreversible Rayleigh coefficients for the PYbN–PT films is shown in Fig. 9. For illustration, Fig. 10 shows the hysteresis at three temperatures for a 0.6 μm thick {100} oriented $0.5PbYb_{1/2}Nb_{1/2}O_3$–$0.5PbTiO_3$ film. For PYbN–PT films, in both film orientations, the reversible Rayleigh parameter increased almost linearly from cryogenic temperatures to T_C. The irreversible Rayleigh parameter also increased with temperature, although for both orientations, at temperatures between ~100 and 250°C, the increase of α' with temperature slowed. At still higher temperatures, the irreversible Rayleigh parameter of the {111} oriented films increased rapidly, reaching values almost double those at room temperature, while the {100} oriented films showed a relatively small increase in α', before it decayed at temperatures around 360°C.

The increase in the reversible Rayleigh parameter with temperature occurs both due to the increase in the intrinsic dielectric permittivity as the films were heated toward T_C, and the increase in the *reversible* domain wall motion

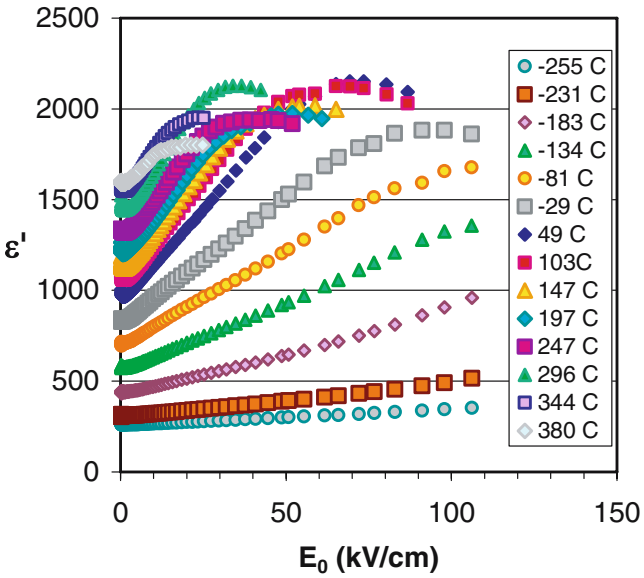

Fig. 8 Temperature dependence of dielectric nonlinearity in {111} oriented PYbN–PT films

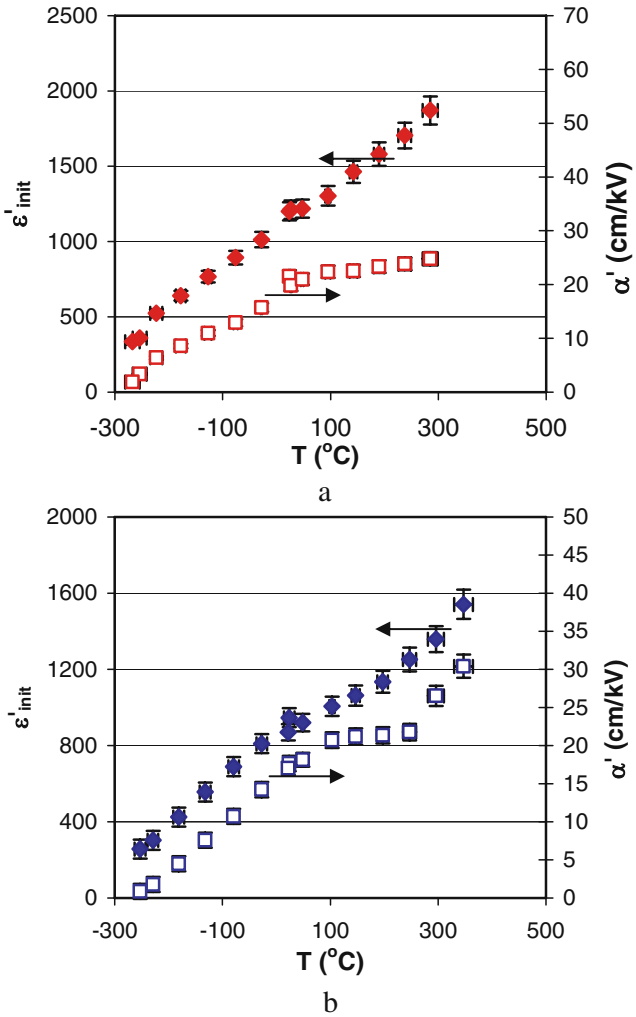

Fig. 9 Temperature dependence of the reversible and irreversible Rayleigh coefficients in (**a**) {100} and (**b**) {111} oriented PYbN–PT at 1 kHz

(along with all other thermally activated processes). This is illustrated schematically in Fig. 11, where we attempt to qualitatively reconstruct the potential profile for a domain wall as a function of temperature. At higher temperatures (well above room temperature), the increased thermal energy makes shallow potential wells less efficient as pinning points for a domain wall. As a result, the energy profile is effectively smoothened, wells are broadened and maxima reduced. This enables larger amplitude, more reversible, domain wall motion (large ε'_{init}) while keeping the nonlinearity also high (large α'). For these films, the broadening of the wells is apparently stronger than the other two process, resulting in a reduction of the irreversible to reversible Rayleigh parameter ratio for temperatures much higher than room temperature, which was confirmed in the experimental results, as shown in Fig. 12.

Results presented in Figs. 9 and 10 indicate that at very low temperatures, ε'_{init} approaches its intrinsic value and extrinsic nonlinearity and hysteresis disappear (α' ap-

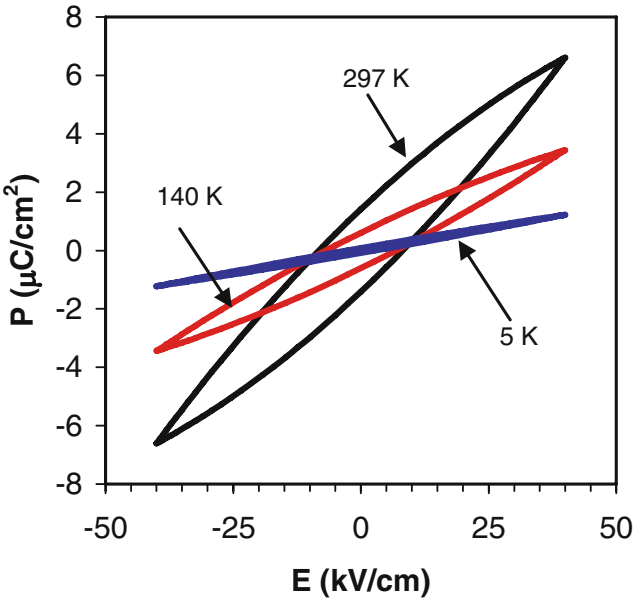

Fig. 10 Polarization hysteresis for a 0.6 μm thick (100) oriented PYbN-PT thin film at 297, 140 and 5 K

proaches zero). The corresponding energy potential for a domain wall could then be represented by deep (reflecting a small or zero α') and narrow (reflecting smaller $\varepsilon'_{\text{init}}$) potential wells, as pictured in Fig. 9a. As temperature increases, the potential evolves, not only due to thermal effects, related changes in domain width and pinning centers' stability, but also because of the driving electric field. The electric field probably increases the roughness of the energy profile, as seen during the transition of acceptor doped PZT ceramics from a hard to a soft state [15, 24]. If, starting with a low temperature, only thermal effects were responsible for the increase in the extrinsic contributions parameters with increasing temperature (Figs. 9 and 10), then the rate-dependent processes would be more pronounced and Rayleigh-like nonlinearity and hysteresis would not dominate at room temperature [17, 25]. Evolution of the energy profile is thus probably determined by coupled and competing effects of thermal activation and profile roughening by the driving field.

It is also expected that the extrinsic nonlinearity should disappear at temperatures higher than T_C due to the loss of domain structure in the paraelectric phase. This could not be confirmed in PYbN–PT or PZT films due to the strong increases in the loss values of the films at temperatures higher than ~300°C. At temperatures around 340°C for the {100} oriented films and ~380°C for the {111} oriented PYbN–PT films, the nonlinear curves began to flatten out, resulting in a reduction of the Rayleigh parameters. This flattening of the nonlinear curves could be due to the steep increase in the loss values of the films at higher temperatures instead of the reduction of the domain wall motion. Separate work on the temperature dependence of the dielectric nonlinearity in $70Pb(Mg_{1/3}Nb_{2/3})O_3$–$30PbTiO_3$ (PMN–PT) thin films with lower loss values near T_C confirmed the reduction of the irreversible Rayleigh parameters beyond the transition temperature (See Fig. 13).

The ratio of the irreversible to reversible Rayleigh parameters seems to be very sensitive to any structural transformations in the films (see Fig. 12). The increase in $\alpha'/\varepsilon'_{\text{init}}$ of {111} oriented films at temperatures around 300–350°C is very probably due to the nearing of the ferroelectric phase transformation. Failure to observe an increase in the Rayleigh parameters of the {100} oriented films might be due to the much higher loss levels observed in this orientation of the PYbN–PN thin films at similar temperatures [60].

Similarly, the relative maximum in the irreversible to reversible Rayleigh parameters ratio at ~100–110°C (corresponding also to a change in the slope of the irreversible Rayleigh parameter vs. temperature at approximately the same temperatures) could be due to the crystallographic phase transformation (rhombohedral to tetragonal) of the material.

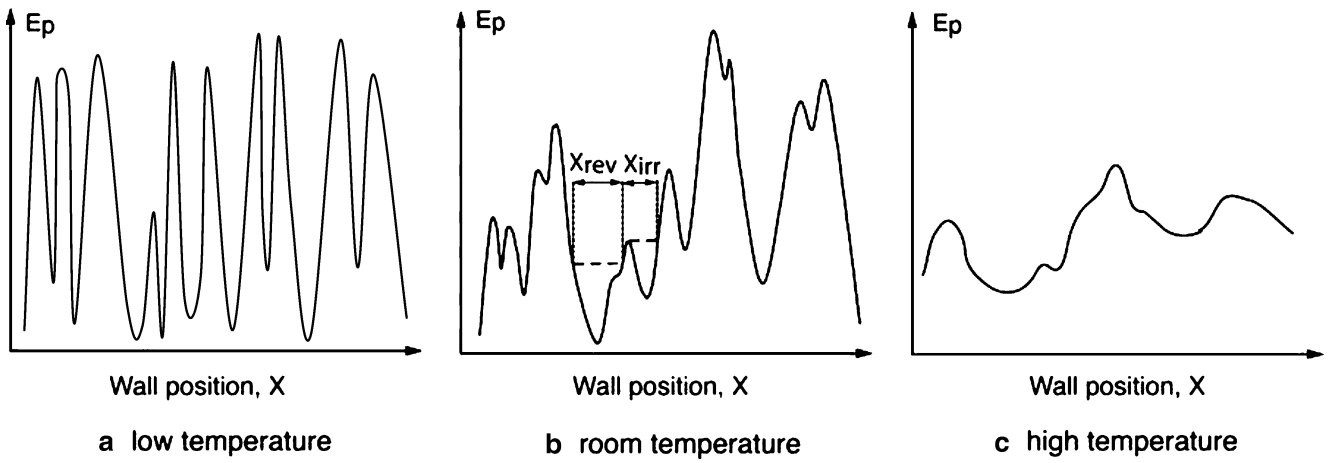

Fig. 11 Schematic comparison of the potential energy profile at (**a**) low temperature, (**b**) around room temperature and (**c**) higher temperatures drawn with respect to the available thermal energy

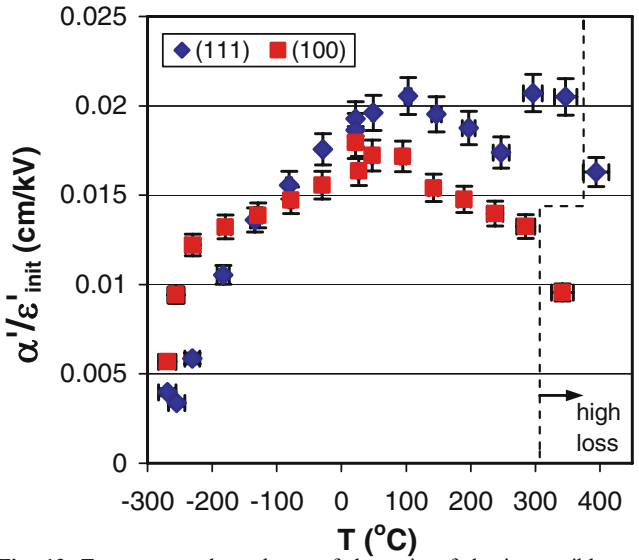

Fig. 12 Temperature dependence of the ratio of the irreversible to reversible Rayleigh parameters in {100} and {111} oriented PYbN–PT thin films at 1 kHz

The change in the increase rate of α' values for temperatures >100–110°C can be then interpreted as a change in either the concentration of the mobile domain walls or their mobility. The strong effect of ferroelectric–ferroelectric phase transitions on the temperature dependence the Rayleigh parameters has been reported for the piezoelectric properties of relaxor-feroelectric single crystals [18].

Another change in the slope of the irreversible to reversible Rayleigh parameters was observed at low temperatures. The temperature at which this variation was observed, $T_{X\rightarrow R}$, was ~−180°C for the {111} oriented thin films and ~−250°C for the {100} oriented PYbN–PT films. The origin of this slope change could be due to a change in the mobility of the domain walls. Intriguingly, in the low field temperature dependence of the dielectric loss for the same films (see Fig. 14), a local maximum was observed at a slightly higher temperature than in the nonlinear measurements. One possibility is that the maximum corresponds to a phase transition of the material from rhombohedral to a different phase. In other perovskite PT-solid solution ferroelectric systems, the presence of a monoclinic or orthorhombic phase close to the MPB has been reported [63–67]. Alternatively, literature reports indicate possible intersection of octahedral tilting transition with the MPB at lower temperatures in other perovskites [68, 69].

It is also worth noting that at ~5K, where the domain wall contribution should be frozen, the ratio of the irreversible to reversible Rayleigh parameters for both of the PYbN–PT thin films' orientations is similar within experimental error.

Although the change of ratio of the irreversible to reversible Rayleigh parameters with temperature seemed to mimic the phase transition of the material as measured by the dielectric permittivity and loss at low field, it was found that the high field characterization reduced the transition temperature with respect to the low field characterization. For example, the rhombohedral to tetragonal phase transformation temperature, $T_{R\rightarrow T}$, as observed in the Rayleigh parameters (see Fig. 15) is 10–50°C lower than the value observed in the low field dielectric permittivity peaks for (100) films [70]. It is likely that phase boundary motion would increase near the phase transition, increasing the irreversible contributions to α'. Field-enhanced phase boundary motion could promote the rhombohedral to tetragonal phase transformation, yielding a lower $T_{R\rightarrow T}$. Similar results have been reported for 0.7PMN-0.3PT thin films: the transition temperature of the films measured at small fields was 30–40°C higher than that measured at higher field [71].

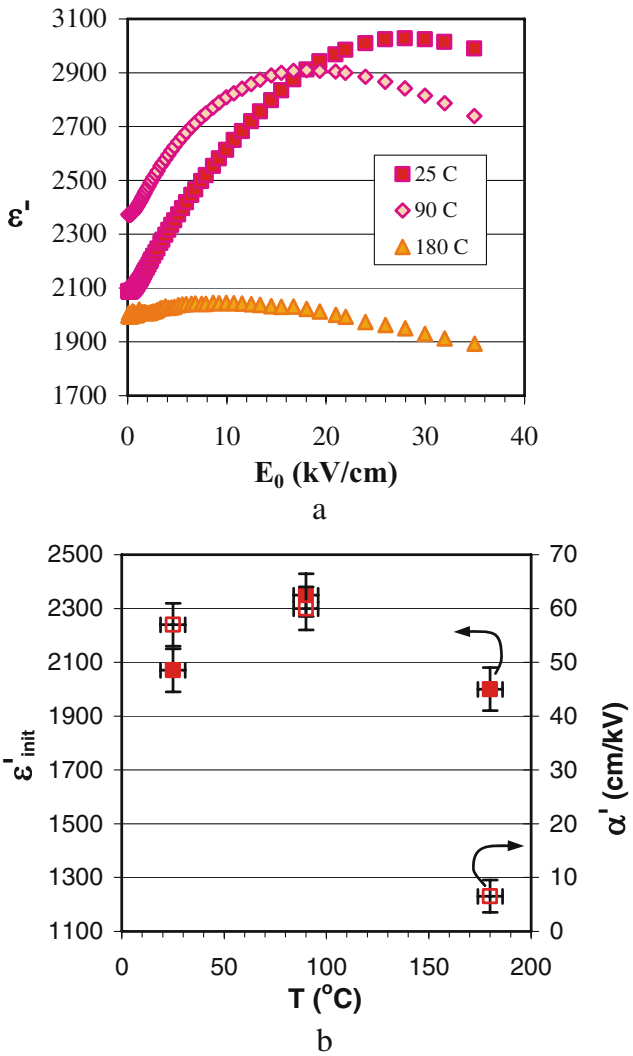

Fig. 13 Temperature dependence of (**a**) dielectric nonlinearity and (**b**) Rayleigh coefficients in PMN–PT thin films

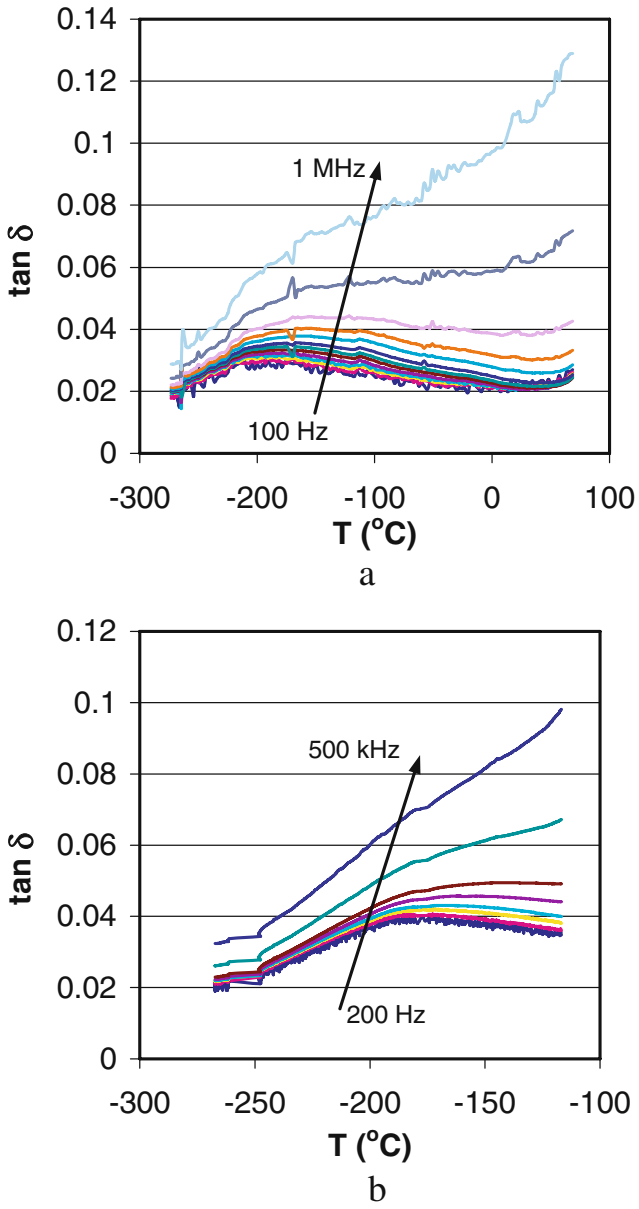

Fig. 14 Temperature dependence of tanδ in (**a**) {100} and (**b**) {111} PYbN-PT films measured at 1 kHz at low fields ($E < E_{th}$)

4 Extrinsic contributions to the piezoelectric response of ferroelectric thin films

In light of the reported low values for the mobility of non-180° domain wall in many ferroelectric thin films (particularly those under a micron in thickness), it would be reasonable to expect that the piezoelectric nonlinearity might be much smaller in thin films than in bulk ceramics of the same composition. Several groups have demonstrated that in many PZT films, this is indeed the case [16, 72].

It is, however, observed, that even in cases where only 180° domain wall motion is present, that domain wall-related piezoelectric nonlinearities can develop in films [73–75]. For example, this situation can occur when there is large-scale, nearly reversible motion of domain walls. Under this situation, the ac field amplitude drives a poling–depoling process that leads to an oscillation of the piezoelectric coefficient: $d_{\text{init}} = d_0[1 + (\beta + \beta' E_0)\sin(\omega t)$, where ω is the angular frequency of the sinusoidal excitation, E_0 is the amplitude of the excitation field, and t is time. β and β' are constants [73]. It is possible to show that this will lead to a linear dependence of the measured piezoelectric coefficient on the amplitude of the applied electric field that corresponds to the Rayleigh law. However, since 180° domain walls are not driven by uniform stresses, this will not result in nonlinearity for the direct piezoelectric coefficient [74]. One consequence of the poling–depoling process is that the amplitude of the second harmonic of the strain response with respect to electric field is larger than that which could be accounted for on the basis of electrostriction. In addition, the second harmonic amplitude is larger than the amplitude of the third harmonic that dominates Rayleigh-like response [4, 33].

4.1 Evidence of Rayleigh-like piezoelectric nonlinearity in PZT thin films

Figure 16 demonstrates typical Rayleigh hysteresis and nonlinearity for the longitudinal converse piezoelectric effect in a {111} oriented 0.9 μm thick 60/40 PZT thin film [78]. Over the examined ac field range, the effective d_{33} increases from 80 to 110 pm/V. Although the relative increase of the piezoelectric coefficient with applied electric

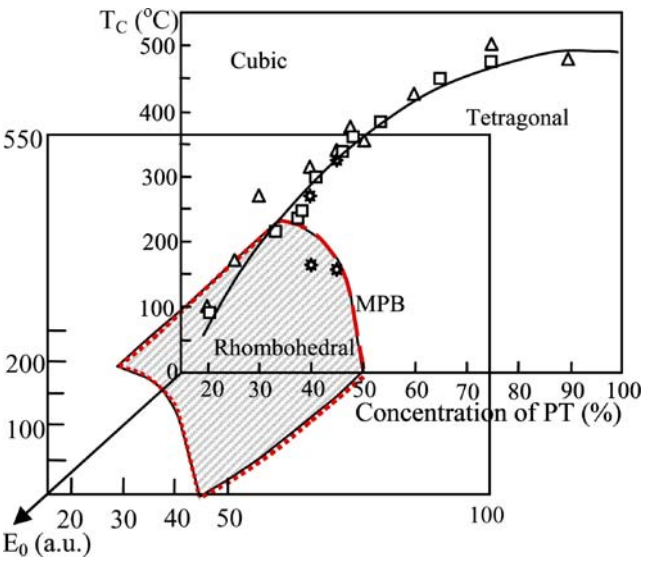

Fig. 15 Schematic representation of the ac field dependence of the MPB curvature in the PYbN–PT system. The change of curvature is exaggerated for clarity. The original phase diagram is after [70]

field in these films is smaller than what would be observed in bulk materials, it is still significant for thin films in which other characterization methods have suggested a limited movement of ferroelastic domain walls [16]. A strong second harmonic (not shown) and the asymmetry in the strain-electric field hysteresis shown in Fig. 16b, indicate a significant contribution to the nonlinearity and hysteresis in this film from displacement of nearly reversible domain wall motion (which may be 180° domain walls, as proposed by the dynamic poling model presented above and in [73, 74]). While a separation of the two contributions could in principle be made using the dynamic poling model, this is out of scope of the present paper.

A systematic investigation of the dynamic piezoelectric effect in textured PZT thin films has shown that the piezoelectric nonlinearity depends on crystal orientation and composition, as seen in Figs. 17, 18 and 19. The results for d_{init} for each examined composition and orientation are in qualitative agreement with predictions of the Landau–Ginzburg–Devonshire (LGD) thermodynamic theory for monodomain single crystals of PZT [76, 77]. Note that, because single crystals of PZT are not available, highly oriented (ideally epitaxial) thin films are presently the only mean of verifying theoretically predicted values of the material coefficients. The trend for nonlinearity, represented by the irreversible coefficient α' is in agreement with the expected domain configuration for each orientation and composition. The results for the tetragonal and morphotropic phase boundary compositions are discussed in some detail below; a discussion on rhombohedral compositions can be found in [78].

In the tetragonal composition, Fig. 17, both d_{init} and α' follow the same trend with respect to the film orientation: $d_{\text{init}}[001] > d_{\text{init}}\{\text{random}\} > d_{\text{init}}\{111\}$ and $\alpha'[100] > \alpha'\{\text{random}\} > \alpha'\{111\}$. These results confirm that the poled tetragonal PZT films with {111} orientation exhibit a special engineered domain configuration (3T) [79], in which all ferroelastic domains are energetically nearly equivalent so that there is no driving force for the domain wall contribution to the piezoelectric effect; ideally, only the dynamic poling process [73, 74] as described above, contributes to the d_{init} and nonlinearity. Considering that the measurements were made under a strong dc bias field, d_{init} for this orientation is dominated by the intrinsic piezoelectric effect reduced by the film clamping effects and augmented by a small contribution from the residual 180° domain walls. Interestingly, unlike in $BaTiO_3$ [80], LGD theory suggests that in all tetragonal compositions of PZT the longitudinal piezoelectric coefficient is largest along the polar axis [001]; hence, $d_{\text{init}}[100] > d_{\text{init}}\{\text{random}\} > d_{\text{init}}\{111\}$ as observed experimentally in the thin films and shown in Fig. 17. The absence of ferroelastic domain wall displacement in {111} oriented film leads to a small α; the small but measurable nonlinearity for this orientation can possibly be attributed to the dynamic poling effects [73].

There are no structural constraints for the displacement of residual 90° domain walls in the [001] oriented films. This orientation thus exhibits appreciable nonlinearity (large α). Figure 17 shows that the d_{init} is largest for this

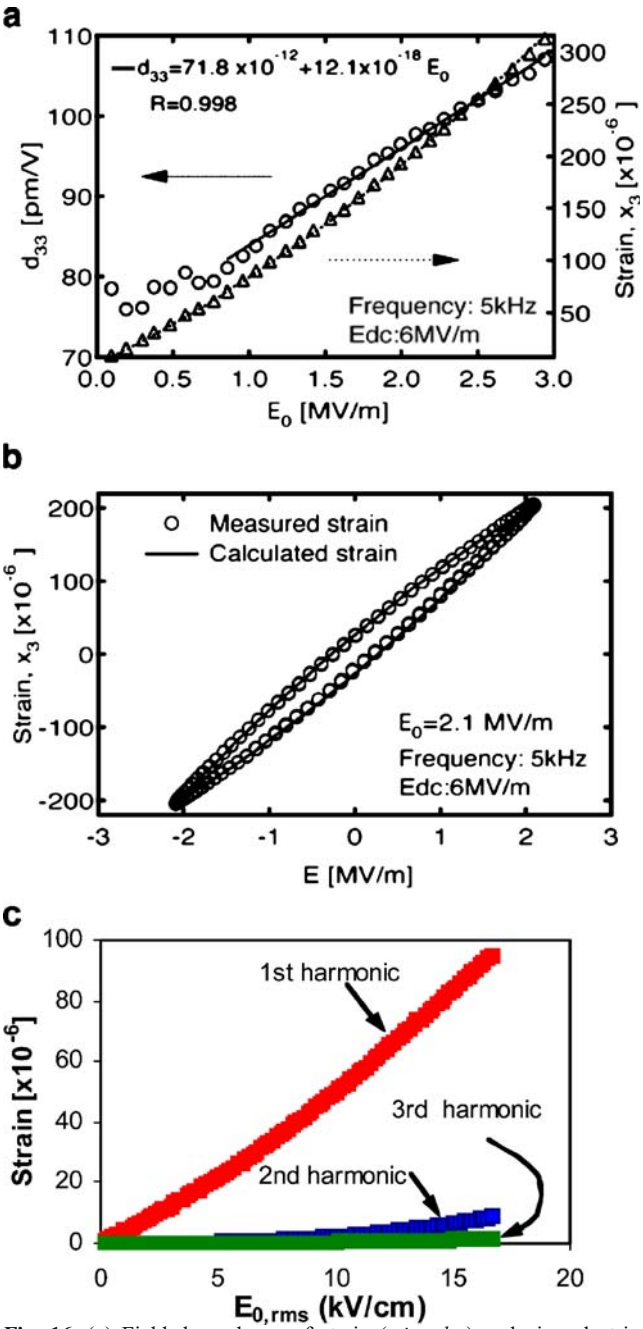

Fig. 16 (**a**) Field dependence of strain (*triangles*) and piezoelectric coefficient (*circles*) for a {111} oriented 0.9 μm thick 60/40 PZT sol–gel deposited thin film. (**b**) A selected strain-electric field loop for E_0= 2.1 MV/m. The *circles* represent experimental data and the *full lines* are calculated using Rayleigh relations and experimental data from (**a**). For details see [78]. (**c**) higher harmonics of strain as a function of applied electric field amplitude for the same film

orientation, which can also be explained by combining effects of both extrinsic and intrinsic contributions. It is interesting that in the PZT solid solution the orientation dependence of d_{33} becomes increasingly isotropic as the MPB is approached from the tetragonal side, leading, close to the MPB, to a d_{33}[001] which is only slightly larger than d_{33}{111} [76]. It is thus tempting to assign the difference between d_{init}[001] and d_{init}{111} mostly to ferroelastic domain wall contributions. However, no definite statements can be made: the coefficients of the LGD function are not very precise near the MPB, and other factors such as substrate clamping or defect concentrations may also be different for the two orientations.

Finally, the randomly oriented tetragonal film shows, as expected, properties somewhere between the two extreme orientations. Taking into consideration all parameters that can influence the piezoelectric properties of the films, it is remarkable that experimental results agree to such a high degree with predictions of the LGD theory and arguments based on the domain configuration.

A similar analysis can be made for the piezoelectric nonlinearity of rhombohedral films, shown in Fig. 18. The orientation dependence of the d_{33} is more anisotropic [76] than for tetragonal films near the MPB, and the difference among d_{init} for the three films is therefore more pronounced. Reflecting the intrinsic piezoelectric anisotropy and domain wall configuration of each orientation, experimental result show that $d_{\text{init}}\{100\} > d_{\text{init}}\{\text{random}\} > d_{\text{init}}\{111\}$ while $\alpha'\{111\} > \alpha'\{\text{random}\} > \alpha'\{100\}$ [76, 78]. At the MPB composition, Fig. 19, both the nonlinearity and d_{init} are similar for the three orientations, this time reflecting the fact that this composition is a mixture of rhombohedral and tetragonal (and potentially monoclinic) phases.

It is interesting that the analysis of the dielectric nonlinearity is more complex because domain walls can contribute to the polarization in films of all orientations and domain wall configurations. In the tetragonal film (Fig. 17), for example, the intrinsic component of the $\varepsilon'_{\text{init}}\{111\}$ should be larger than that of the $\varepsilon'_{\text{init}}[001]$. It is a common feature of most perovskites that the permittivity is smallest along the polar direction, and largest perpendicular to it. The experimental data from Fig. 17 show that $\varepsilon'_{\text{init}}[001] > \varepsilon'_{\text{init}}[111]$, suggesting that extrinsic contributions dominate permittivity for the film with [001] orientation. Again, one cannot ignore the possibility that other factors, such as a different degree of film clamping by the substrate may influence the difference in $\varepsilon'_{\text{init}}$ for the orientations examined.

4.2 Piezoelectric response of thin films under DC bias

One commonly used method of characterization of thin films is to measure the effective piezoelectric response (usually d_{33}) as a function of dc bias electric field. As in the case of the ac driving fields, the resulting nonlinearity is controlled by both intrinsic and extrinsic contributions. The expected intrinsic component can be readily modeled by the LGD theory [11]. While experimentally one nearly always measures the piezoelectric response under both positive and negative biases, the theoretical calculations of Chen et al. [11] considered positive bias only. LGD theory predicts that the piezoelectric coefficients and permittivity in perovskite materials will initially increase with an applied negative bias (until depoling and repoling set in), as shown in Fig. 20 for the longitudinal piezoelectric coefficient of a tetragonal PZT [12, 81]. An increasing d_{33} at modest negative bias fields has been observed both in bulk materials [82] and in thin films [83]. However, even in those cases the response is probably not controlled by intrinsic effects alone.

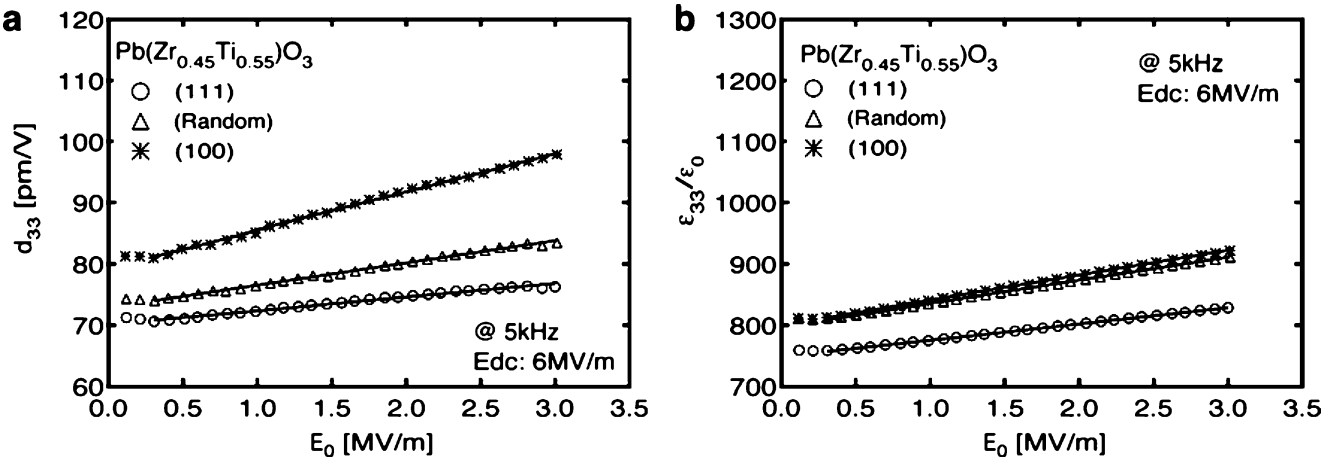

Fig. 17 Orientation dependence of (**a**) piezoelectric coefficient and (**b**) relative dielectric permittivity as a function of ac field amplitude in sol–gel prepared 0.9 μm thick tetragonal PZT 45/55 films. The *full lines* are fits to Rayleigh equation. Note that a dc bias of 6 MV/m was applied on the film during measurements. For details see [78]

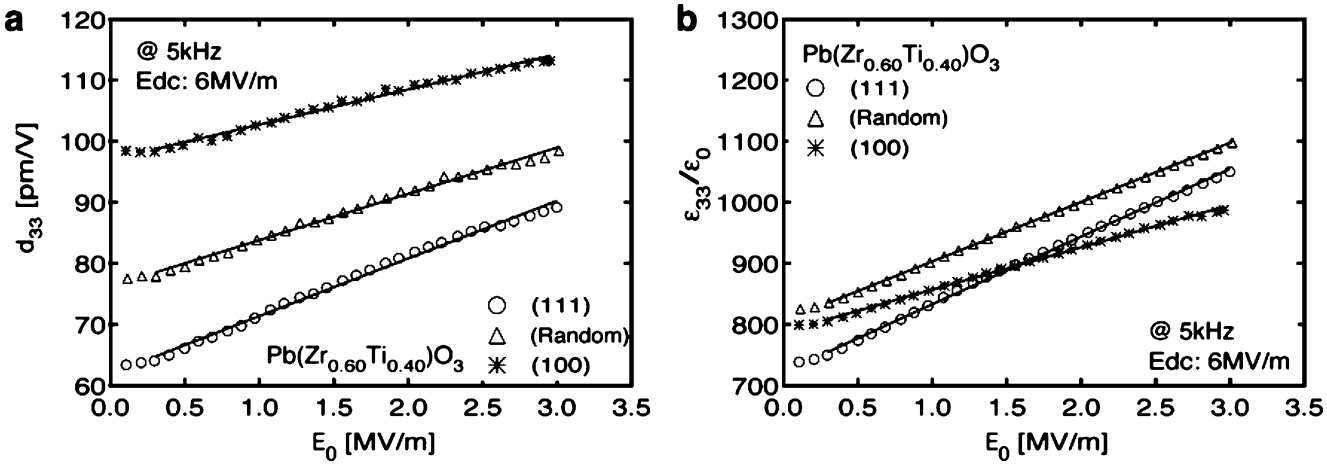

Fig. 18 Orientation dependence of (**a**) piezoelectric coefficient and (**b**) relative dielectric permittivity as a function of ac field amplitude in sol–gel prepared 0.9 μm thick rhombohedral PZT 60/40 films. The *full lines* are fits to the Rayleigh equation. Note that a dc bias of 6 MV/m was applied on the film during measurements. For details see [78]

Interpretation of the d–E_{dc} loops is nontrivial. Tagantsev et al. [75] have proposed a model to explain why in some case the d–E_{dc} loop rotates clockwise at high dc bias fields. Their explanation that the clockwise rotation is due to the switching of 180° domain walls only is restrictive because the same effect was reported for the d_{33} vs. compressive pressure loops in ceramics [84], which is most likely caused by ferroelastic (non-180°) domain switching. It may be germane to many thin films, however, given the limited mobility of ferroelastic walls.

The d–E_{dc} loops are controlled by the polarization state of the ferroelectric, and are thus strongly sensitive to the fatigue state of the sample [85, 86]. Large qualitative changes in the shape of the loops can be observed sometimes after only few cycles, as seen in Fig. 21. For illustration of the different processes that can contribute to the piezoelectric response, the loops taken during the first and the last cycle are analyzed below.

During the first cycle, the film is first polarized as E_{dc} is increased from zero to its maximum value (not shown). When E_{dc} is subsequently decreased from its maximum positive value, two effects can be responsible for the increasing d_{33}. First, as already indicated, the intrinsic d_{33} is suppressed at high E_{dc}, see Fig. 20. Therefore, when E_{dc} decreases, d_{33} increases. Second, if a poled film still contains residual domains at its maximum E_{dc}, the domain walls will be displaced by the driving E_{ac} field contributing to the d_{33}. This dynamic motion of domain walls, as discussed earlier for the dielectric permittivity, is limited at large E_{dc} and becomes more significant as the E_{dc} is

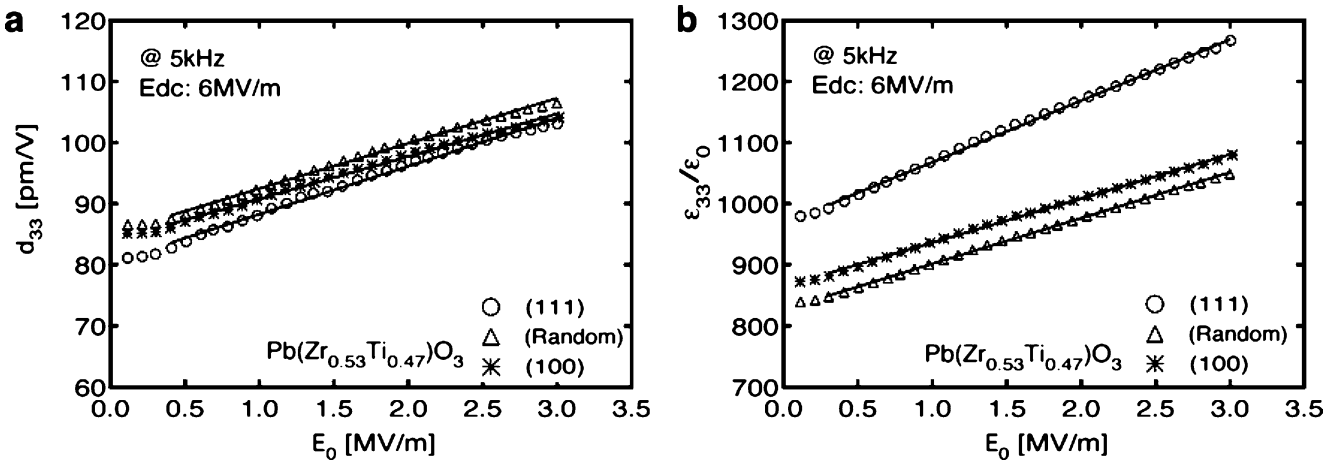

Fig. 19 Orientation dependence of (**a**) piezoelectric coefficient and (**b**) relative dielectric permittivity as a function of ac field amplitude in sol–gel prepared, 0.9 μm thick, morphotropic phase boundary PZT 53/47 films. The *full lines* are fits with Rayleigh equation. Note that a dc bias of 6 MV/m was applied on the film during measurements. For details see [78]

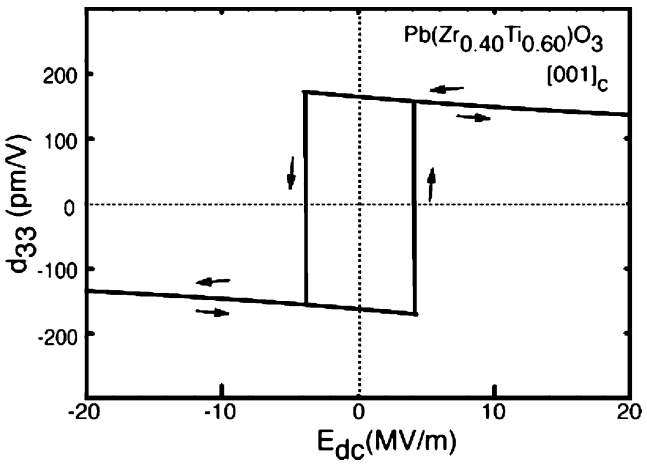

Fig. 20 Longitudinal peizoelectric coefficient of a tetragonal PZT monodomain single crystal as a function of dc bias electric field calculated by the LGD theory. The *arrows* indicate sense of the loop rotation. Qualitatively similar behavior is expected for rhombohedral and MPB compositions with various orientations. The coercive field is arbitrarily chosen to be of the same order of magnitude as that observed experimentally in PZT thin films. For details see [85]

reduced toward zero; thus, d_{33} increases due to a combination of intrinsic and extrinsic contributions. At E_{dc} fields close to zero d_{33} decreases. This is due to back-switching of domains: some domains reoriented by the bias field will back-switch near zero E_{dc}, Both 180° and ferroelastic domain walls may back-switch. The fact that the d_{33} starts decreasing close to zero E_{dc} is thus contrary to intrinsic behavior and a clear indication that extrinsic contributions control the shape of the d_{33}–E_{dc} loop. This is not, however, always the case and there are reports [83] which show that the d_{33} continues increasing as E_{dc} decreases and becomes negative (i.e. opposing the existing polarization), indicating a stable domain structure.

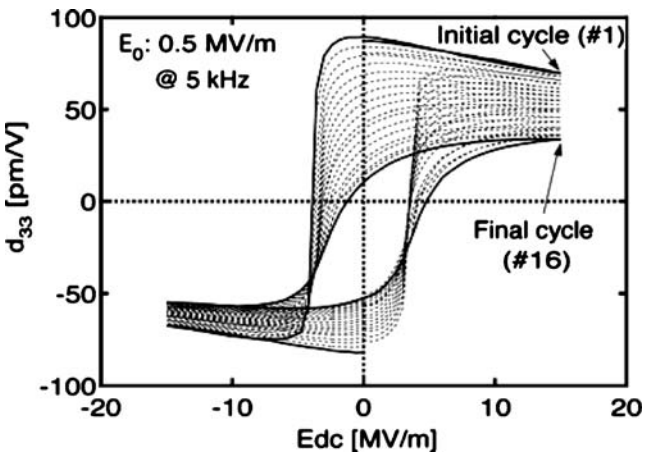

Fig. 21 Evolution of the d_{33}–E_{dc} loop in a 1.44 μm thick (111) oriented sol–gel derived 45/55 PZT film with number of dc field cycles. For details see [78] and [87]

In the fatigued state (the last cycle in Fig. 21) the d_{33}–E_{dc} loop is strongly slanted. Domain reorientation is blocked by strong elastic and/or electric restoring fields that have developed in the film during the fatigue process and the domain wall contribution to the dynamic piezoelectric response becomes small. In addition, while the large E_{dc} can reverse domains, as seen by an increasing d_{33} with increasing E_{dc}, the domains switch back immediately after the dc field is reduced, confirming the presence of the strong domain wall pinning and associated restoring forces in the fatigued state.

The d_{33}–E_{dc} loops for three compositions and three different orientations of PZT films are shown in Fig. 22. In

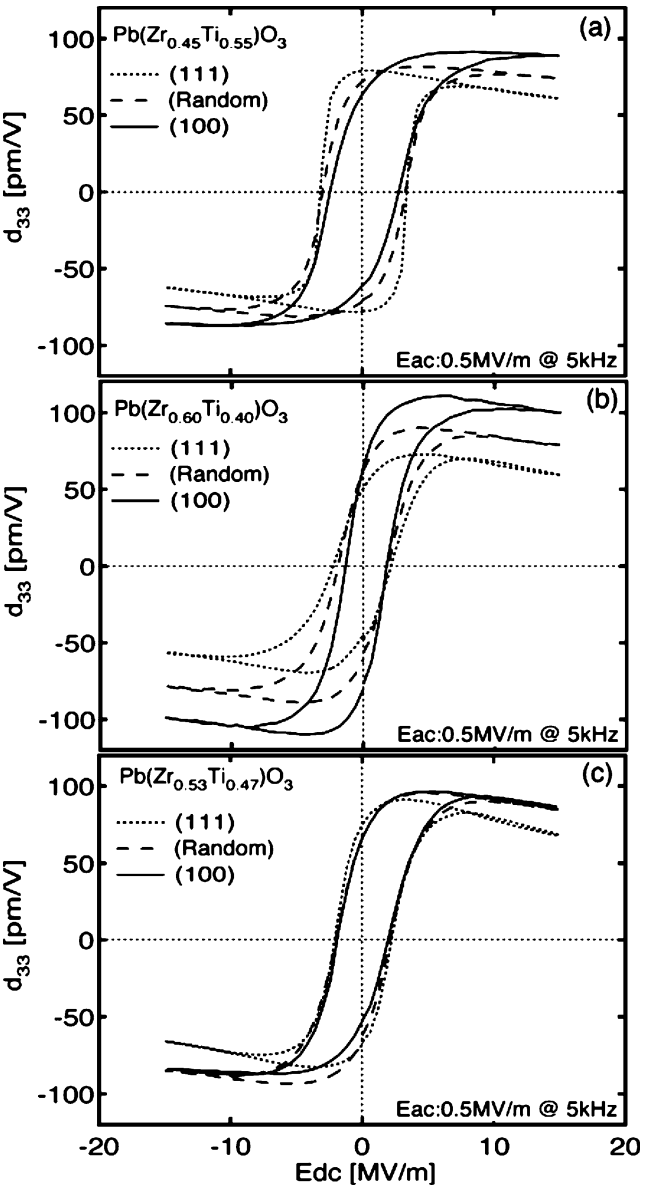

Fig. 22 Orientation dependence of the piezoelectric coefficient as a function of dc electric bias field in 0.9 μm thick (**a**) 45/55 PZT film, (**b**) 60/40 PZT film and (**c**) 53/47PZT film. For details see [78]

the case of the tetragonal film, Fig. 22a, there is a clear and qualitative difference between the loops for the {001} and {111} oriented films. It is tempting to associate the differences in the amount of backswitching with the film orientation. The arguments would be the following. The back switching is weakest in the {111} textured film, which may be expected because there should be no large elastic driving forces to switch between three nearly equivalent [87] ferroelastic domain walls. In the {001} film, the back switching is strongest because 90° domain wall switching can significantly change the elastic energy balance: those domain walls that are switched by the strong E_{dc} will switch back as soon as the field is reduced to release the elastic strain associated with the tetragonal distortion of the material. However, the presented arguments are certainly not valid in the general case, as shown for rhombohedral PZT films (with a Zr/Ti ratio of 60/40), where all three examined orientations exhibit a similar degree of back-switching and qualitatively identical loops (see Fig. 22b). There are many processes that can affect backswitching in films. For example, even slight differences in the film preparation may lead to different chemistry at the film surface (e.g., different lead stoichiometry) that could have a stronger effect on backswitching than the film orientation.

5 Conclusions

Piezoelectric thin films based on ferroelectric compositions show extrinsic contributions to the dielectric and piezoelectric properties that can be a significant fraction of the measured responses at room temperature. For modest excitation levels, provided that the link between nonlinearity and hysteresis is verified, the Rayleigh approach provides a useful means of quantifying the magnitude of the extrinsic contributions. It is found that thin films often show substantially smaller extrinsic contributions to the piezoelectric response than do bulk ceramics of the same composition. It is believed that the small grain sizes, substantial residual stresses, and the high concentration of point and line defects reduce the relative mobility of the domain and phase boundaries.

Acknowledgements This work was supported by the Office of Naval Research (grant N00014-96-C-0387), the National Science Foundation (through grants DMR-0213623, DMR-0313764, and DMR-0602770), and the Center for Dielectric Studies at the Pennsylvania State University (STM); and the Swiss National Science Foundation (DD). The authors also gratefully acknowledge that some substrates were provided by Dr. P. Muralt (EPFL).

References

1. J.L. Jones, M. Hoffman, J.E. Daniels, A.J. Studer, Appl. Phys. Lett. **89**, 092901 (2006)
2. D.A. Hall, J. Mater. Sci. **36**, 4575 (2001)
3. D.V. Taylor, D. Damjanovic, J. Appl. Phys. **82**, 1973 (1997)
4. D.V. Taylor, D. Damjanovic, Appl. Phys. Lett. **73**, 2045 (1998)
5. D.V. Taylor, D. Damjanovic, N. Setter, Ferroelectrics **224**, 299 (1999)
6. M.E. Lines, A.M. Glass, *Principles and Applications of Ferroelectrics and Related Materials* (Oxford University Press, New York, 1977)
7. S. Stemmer, S.K. Streiffer, F. Ernst, M. Rühle, Philos. Mag., A **71**, 713 (1995)
8. R. Herbiet, U. Robels, H. Dederichs, G. Arlt, Ferroelectrics **98**, 107 (1989)
9. An American National Standard IEEE Standard Definitions of Terms Associated with Ferroelectric and Related Materials, IEEE Trans. Ultrason. Ferroelectr. Freq. Control **50**, 1 (2003)
10. S. Li, W. Cao, L.E. Cross, J. Appl. Phys. **69**, 7219 (1991)
11. L. Chen, V. Nagarajan, R. Ramesh, A.L. Roytburd, J. Appl. Phys. **94**, 5147 (2003)
12. M. Budimir, D. Damjanovic, N. Setter, Appl. Phys. Lett. **85**, 2890 (2004)
13. L. Rayleigh, Philos. Mag. **23**, 225 (1887)
14. L. Néel, Cah. Phys. **12**, 1 (1942)
15. D. Damjanovic, in *Hysteresis in Piezoelectric and Ferroelectric Materials*, eds. by G. Bertotti, I. Mayergoyz. Science of Hysteresis, vol III (Elsevier, 2005), p. 337
16. F. Xu, S. Trolier-McKinstry, W. Ren, B. Xu, Z.L. Xie, K.J. Hemker, J. Appl. Phys. **89**, 1336 (2001)
17. D. Damjanovic, J. Appl. Phys. **82**, 1788 (1997)
18. M. Davis, D. Damjanovic, N. Setter, J. Appl. Phys. **100**(8), 084103 (2006)
19. J.E. García, R. Pérez, A. Albareda, J. Phys., Condens. Matter **17**, 7143 (2005)
20. H. Kronmüller, Z. Angew. Phys. **30**, 9 (1970)
21. G. Robert, D. Damjanovic, N. Setter, A.V. Turik, J. Appl. Phys. **89**, 5067 (2001)
22. G. Robert, D. Damjanovic, N. Setter, J. Appl. Phys. **90**, 2459 (2001)
23. G. Arlt, H. Dederichs, R. Herbeit, Ferroelectrics **74**, 37 (1987)
24. M. Morozov, D. Damjanovic, N. Setter, J. Eur. Ceram. Soc. **25**, 2483 (2005)
25. G. Robert, D. Damjanovic, N. Setter, J. Appl. Phys. **90**, 4668 (2001)
26. D. Damjanovic, M. Demartin, J. Phys., Condens. Matter **9**, 4943 (1997)
27. L.X. Zhang, X.B. Ren, Phys. Rev., B **73**, 094121 (2006)
28. U. Robels, G. Arlt, J. Appl. Phys. **73**, 3454 (1993)
29. O. Boser, J. Appl. Phys. **62**, 1344 (1987)
30. H.J. Hagemann, J. Phys. C. Solid State Phys. **11**, 3333 (1978)
31. L. Sagalowicz, F. Chu, P. Duran Martin, D. Damjanovic, J. Appl. Phys. **88**, 7258 (2000)
32. M. Davis, D. Damjanovic, N. Setter, (unpublished) (2006)
33. T.M. Shaw, S. Trolier-McKinstry, P.C. McIntyre, Annu. Rev. Mater. Sci. **30**, 263 (2000)
34. W. Cao, C. Randall, J. Phys. Chem. Solids **57**, 1499 (1996)
35. G. Arlt, N.A. Pertsev, J. Appl. Phys. **70**, 2283 (1991)
36. B. Jaffe, W.R. Cook Jr., H. Jaffe, *Piezoelectric Ceramics* (Academic, re-printed in India, 1971)
37. A.Y. Emelyanov, N.A. Pertsev, Phys. Rev., B **68**, 214103 (2003)
38. V.G. Koukhar, N.A. Pertsev, R. Waser, Phys. Rev., B **64**, 214103 (2001)
39. B.A. Tuttle, T.J. Garino, J.A. Voight, T.J. Headley, D. Dimos, M. O. Eatough. in *Science and Technology of Electroceramic Thin*

Films, eds. by O. Auciello, R. Waser (Kluwer, The Netherlands, 1995), pp. 117–1132
40. K.S. Lee, Y.K. Kim, S. Baik, J. Kim, I.S. Jung, Appl. Phys. Lett. **79**, 2444 (2001)
41. M.B. Kelman, P.C. McIntyre, B.C. Hendrix, S.M. Bilodeau, J.F. Roeder, J. Appl. Phys. **93**, 9231 (2003)
42. J.F. Shepard Jr., F. Chu, B. Xu, S. Trolier-McKinstry, *in MRS Proc.: Ferroelectric Thin Films VI***493**, 69 (1998)
43. N. Bassiri Gharb, P. Muralt, S. Trolier McKinstry, in *Proceedings 14th IEEE Int. Symp. Appl. Ferroelectrics*, 95 (2004)
44. Z. Zhang, J.-H. Park, S. Trolier-McKinstry, *MRS. Proc. Ferroelectric Thin Films VIII*, eds. by R.W. Schwartz, P.C. McIntyre, Y. Miyasaka, S.R. Summerfelt, D. Wouters, vol. 596 (Materials Research Society, Warrendale, PA, 2000), pp. 73–77
45. F. Xu, S. Trolier-McKinstry, W. Ren, B. Xu, J. Appl. Phys. **89**, 1336 (2001)
46. S. Trolier-McKinstry, J.F. Shepard Jr., J.L. Lacey, T. Su, G. Zavala, J. Fendler, Ferroelectrics **206–207**, 381 (1998)
47. A.L. Kholkin, K.G. Brooks, N. Setter, Appl. Phys. Lett. **71**, 2044 (1997)
48. N.A. Pertsev, A.Y. Emelyanov, Appl. Phys. Lett. **71**, 3646 (1997)
49. G. Bertotti, *Hysteresis in Magnetism* (Academic, San Diego, 1998)
50. J.E. Garcia, R. Perez, A. Albareda, J. Phys., D. Appl. Phys. **34**, 3279 (2001)
51. H.H.A. Krueger, J. Acoust. Soc. Am. **42**, 636 (1967)
52. D. Damjanovic, S.S.N. Bharadwaja, N. Setter, Mater. Sci. Eng., B **120**, 170 (2005)
53. Z. Kighelman, D. Damjanovic, M. Cantoni, N. Setter, J. Appl. Phys. **91**, 1495 (2002)
54. K.M. Johnson, J. Appl. Phys. **33**, 2826 (1962)
55. C. Ang, Z. Yu, Appl. Phys. Lett. **85**, 3821 (2004)
56. C. Ang, Z. Yu, Phys. Rev., B **69**, 174109 (2004)
57. R.A. Wolf, S. Trolier-McKinstry, J. Appl. Phys. **95**, 1397 (2004)
58. E. Hong, R. Smith, S.V. Krishnaswamy, C.B. Freidhoff, S. Trolier-McKinstry, IEEE Trans. Ultrason. Ferroelectr. Freq. Control **53**, 697 (2006)
59. X.L. Zhang, Z.X. Chen, L.E. Cross, W.A. Schulze, J. Mater. Sci. **18**, 968 (1983)
60. N. Bassiri Gharb, S. Trolier-McKinstry, J. Appl. Phys. **97**, 064106 (2005)
61. D.A. Hall, M.M. Ben-Omran, J. Phys., Condens. Matter **10**, 9129 (1998)
62. S.-M. Nam, Y.-B. Kil, S. Wada, T. Tsurumi, Jpn. J. Appl. Phys. **42**, L1519 (2003)
63. B. Noheda, D.E. Cox, G. Shirane, J.A. Gonzalo, L.E. Cross, S.-E. Park, Appl. Phys. Lett. **74**, 2059 (1999)
64. Y. Lu, D.-Y. Jeong, Z.-Y. Cheng, Q.M. Zhang, H.S. Luo, Z.Y. Yin, D. Viehland, Appl. Phys. Lett. **78**, 3109 (2001)
65. Y. Guo, H. Luo, T. He, H. Xu, Z. Yin, Jpn. J. Appl. Phys. **41**, 1 (2000)
66. K. Fujishiro, R. Vlokh, Y. Uesu, Y. Yamada, J.-M. Kiat, B. Dkhil, Y. Yamashita, Jpn. J. Appl. Phys. **37**, 5246 (1998)
67. M.K. Durbin, J.C. Hicks, S.-E. Park, T.R. Shrout, J. Appl. Phys. **87**, 8159 (2000)
68. R.E. Eitel, S.J. Zhang, T.R. Shrout, C.A. Randall, I. Levin, J. Appl. Phys. **96**, 2828 (2004)
69. H. Zheng, I.M. Reaney, W.E. Lee, H. Thomas, N. Jones, J. Am. Ceram. Soc. **85**, 2337 (2002)
70. S. Zhang, P.W. Rehrig, C. Randall, T.R. Shrout, J. Cryst. Growth **234**, 415 (2002)
71. A. Laha, S.B. Krupanidhi, Mater. Sci. Eng., B **113**, 190 (2004)
72. A.L. Kholkin, M.L. Calzada, P. Ramos, J. Mendiola, N. Setter, Appl. Phys. Lett. **69**, 3602 (1996)
73. S. Trolier-McKinstry, N. Bassiri Gharb, D. Damjanovic, Appl. Phys. Lett. **88**, 202901 (2006)
74. N. Bassiri Gharb, S. Trolier-McKinstry, D. Damjanovic, J. Appl. Phys. **100**, 044107 (2006)
75. T. Tagantsev, P. Muralt, J. Fousek, Mater. Res. Soc. Symp. Proc. **784**, 517 (2004) (C10.6.1)
76. D. Damjanovic, J. Am. Ceram. Soc. **88**, 2663 (2005)
77. M.J. Haun, E. Furman, S.J. Jang, L.E. Cross, Ferroelectrics **99**, 63 (1989)
78. D.V. Taylor, D. Damjanovic, Appl. Phys. Lett. **76**, 1615 (2000)
79. M. Davis, D. Damjanovic, D. Hayem, N. Setter, J. Appl. Phys. **98**, 014102 (2005)
80. S. Wada, S. Suzuki, T. Noma, T. Suzuki, M. Osada, M. Kakihana, S.-E. Park, L.E. Cross, T.R. Shrout, Jpn. J. Appl. Phys. **38**, 5505 (1999)
81. N. Setter, D. Damjanovic, L. Eng et al., J. Appl. Phys. **100**, 051606 (2006)
82. Y. Zhang, I.S. Baturin, E. Aulbach, D.C. Lupascu, A.L. Kholkin, Y.V. Shur, J. Rödel, Appl. Phys. Lett. **86**, 012910 (2005)
83. S. Yokoyama, Y. Honda, H. Morioka, S. Okamoto, H. Funakubo, T. Iijima, H. Matsuda, K. Saito, T. Yamamoto, H. Okino, O. Sakata, S. Kimura, J. Appl. Phys. **98**, 094106 (2005)
84. H.H.A. Krutger, "Stress sensitivity of piezoelectric ceramics: Part 1. Sensitivity to compressive stress parallel to the polar axis," Technical publication TP-242-1: Stress sensitivity of piezoelectric ceramics, Morgan Electro Ceramics; http://www.morganelectroceramics.com/techpub1.html
85. E.L. Colla, D.V. Taylor, A.K. Tagantsev, N. Setter, Appl. Phys. Lett. **72**, 2478 (1998)
86. A.L. Kholkin, E.L. Colla, A.K. Tagantsev, D.V. Taylor, Appl. Phys. Lett. **68**, 2577 (1996)
87. M. Davis, D. Damjanovic, N. Setter, Appl. Phys. Lett. **87**, 102904 (2005)